Study of high-lying cluster states of nuclei by the method of particle–particle angular correlations

T. L. Belyaeva and N. S. Zelenskaya
Skobel'tsyn Institute of Nuclear Physics, Moscow State University

Fiz. Élem. Chastits At. Yadra **29**, 261–332 (March–April 1998)

The current status of research on nuclear reactions induced by light and semiheavy ions of energy up to 10 MeV/nucleon on light and intermediate nuclei by measurement of the angular correlation functions of the final products is reviewed. The principal theoretical and experimental studies on particle–particle correlations carried out in recent years are analyzed. The methods of calculating the angular correlation functions and the spin tensors of the reaction-product density matrix for reactions involving excited states using the distorted-wave method with finite interaction range and the modified compound-nucleus model are described. The $\alpha-d$ and $\alpha-t$ correlations in reactions involving ^{6,7}Li and ^{14}N ions are analyzed. The highly excited α-cluster states in ^{12}C, ^{16}O, ^{20}Ne, and ^{24}Mg are studied. The polarization tensors of the ^{6}Li nucleus in the 3^+ state are calculated and compared with experiment. It is shown that the particle–particle angular correlation functions and the polarization tensors can provide unique information about the reaction mechanism and about the structure of the wave functions of highly excited nuclear states, including the nature of the radial dependence in the interior of the nucleus and the optical interaction potentials in the entrance and exit reaction channels, and so on. This review can be useful for both theoreticians and experimentalists working on the physics of nuclear reactions involving particles of moderate energy.
 [S1063-7796(98)00102-8]

1. INTRODUCTION

According to quantum mechanics, the wave function of a particle with spin I depends on the spin variable: the projection M_I of the spin on the specified quantization axis z, which can take $2I+1$ discrete values. For an unperturbed nuclear system the substates with various M_I are uniformly populated, and the spatial orientation of the spin is isotropic. Nuclear systems in which the spatial orientation of the particle spins is not isotropic are termed oriented.

In a collision of particles possessing spins, the interaction is in general noncentral, i.e., it depends on the relative orientation of the spins and on the relative separation vector. Therefore, nuclear reaction products whose spatial distribution is anisotropic are oriented systems, and the nuclear reaction itself plays the role of a "polarizer." In particular, if the mechanism for final-particle formation is different from statistical evaporation from a state of thermodynamical equilibrium, the final nucleus (which possesses nonzero spin) is oriented, and the populations of the substates with different M_I are nonuniform. If the final nucleus is formed in an excited state, its decay is also anisotropic. Then the angular distribution of the decay products will be determined by the probability for populating the various substates of the final nucleus, i.e., by the nuclear spin orientation.

On the other hand, the study of the angular dependence of the populations of the various substates makes it possible to identify the reaction mechanisms, because different mechanisms are manifested to different degrees depending on the emission angle of the final particle, and this is reflected in the angular dependence of the population of the various substates.

A popular method of obtaining information about the properties of oriented systems is the study of the angular correlation functions of the reaction products. This method has been used to obtain valuable experimental data on the properties of nuclei and their excited states, on nuclear interactions, and on nuclear reaction mechanisms.

The analysis of all types of angular correlation involves the use of a theoretical technique based on the spin density matrix developed in Refs. 1–3 and described in greatest detail in the review by Goldfarb.[4] Many questions related to the study of polarization phenomena in nuclear reactions are discussed in Ref. 5. A recent monograph[6] proposes and theoretically justifies a method of determining the spin characteristics of nuclear states based on measurement of the particle–reaction-product angular correlation functions and the radiation emitted by the nucleus in an excited state measured in various planes.

The study of correlations of the particle–particle type historically began with quasielastic knockout reactions $A(p,2p)B^*$ (Ref. 7) on light nuclei at incident proton energies of 150–200 MeV. The momentum distributions and excitation spectra of the final nuclei in these reactions were described theoretically by Balashov *et al.*[8] The further experimental and theoretical study of (a,ax) reactions in the quasielastic kinematics made it possible to study the clustering of light nuclei.[9] A detailed analysis of the experimental data on such reactions can be found in Ref. 10.

The interesting regularities in the angular correlations of

the final particles from reactions induced by lithium ions and α particles (decay products of the excited state of the final nucleus) have been studied by Ogloblin, Goldberg *et al.*[11–13] The analysis of these data showed that the study of angular correlations in direct α-transfer reactions can be used to determine both the spin characteristics of high-lying excited α-cluster states, and the parameters of the nuclear interaction potentials in the excited state.

The study of the angular correlations in multinucleon transfer reactions[14–16] opens up new possibilities in the study of quasimolecular nuclear states with high spin, the more detailed study of the mechanisms of such reactions, and of the structure and spectroscopy of excited states containing 2α and 3α clusters.

A very important problem is the experimental and theoretical study of the polarization tensors of excited nuclear states, whose angular distributions can be obtained directly from the experimental angular correlation functions measured under special kinematical conditions. The method of reconstructing the complete nuclear spin density matrix proposed and realized at the Institute of Nuclear Physics, Moscow State University[17–19] by studying the particle–γ angular correlation functions has allowed the detailed investigation of the orientational characteristics of the lowest excited states of the ^{12}C, ^{16}O, ^{32}S, etc., nuclei.[20–23] Similar techniques for reconstructing the components of the polarization tensors of excited states of light nuclei in studying the particle–particle angular correlation functions have been used in Refs. 24 and 25.

In this review we give a detailed discussion of the problems associated with analyzing the recent results of experimental and theoretical studies of particle–particle angular correlations. We use them to study the properties of oriented systems and high-lying cluster states and their production mechanisms.

2. THE SPIN DENSITY MATRIX AND ITS SPIN TENSORS IN BINARY NUCLEAR REACTIONS

We shall analyze the differential cross sections and angular correlation functions in reactions involving light and semiheavy ions, using the general theory of angular correlations[4,19,24] in terms of the spin density matrix $\rho_I(M_f,M_f')$ of the nuclear state with spin I_f and its spin tensors $\rho_{k\varkappa}(I_f)$. The density matrix, which was first introduced into theoretical physics by Landau, allows the analytic construction of general expressions, the calculation of the expectation value of any physical quantity, and the unique description of both completely and incompletely defined quantum-mechanical states. The concept of the density matrix has been developed by many authors; here we shall refer to the fundamental monographs of Refs. 25 and 26.

The spin density matrix, or the density matrix in spin variables, characterizes the orientational characteristics of a system and can be obtained from the complete wave function $\Psi_I(\mathbf{r},M)$ of a system of spin I by integration over the radial variable:

$$\rho_I(M,M')=\int d^3\mathbf{r}|\Psi_I(\mathbf{r},M')\rangle\langle\Psi_I(\mathbf{r},M)|. \tag{1}$$

The diagonal elements of the spin density matrix give the probability that the system is found in a state with a given spin projection M, i.e., these elements determine the orientation of the system in spin space. The sum of the diagonal elements is given by the normalization condition:

$$\mathrm{Tr}\,\rho_I(M,M)=1. \tag{2}$$

In a nonoriented system all the spin states are populated with equal probability:

$$\rho_I(M,M')=\frac{\delta_{MM'}}{2I+1}. \tag{3}$$

The spin tensors of the density matrix are more convenient than the spin density matrix for practical applications. Using the fact that the elements of the spin density matrix transform under rotations of the coordinate system like the direct product of two irreducible representations of the rotation group, we can define the spin tensors of the density matrix as

$$\rho_{k\varkappa}(I_f)=\sqrt{2I_f+1}\sum_{M_fM_f'}(-1)^{I_f-M_f'}\times\langle I_fM_f'I_f-M_f|k\varkappa\rangle\rho_{I_f}(M_f,M_f'), \tag{4}$$

where $0<k<2I_f$ and $\varkappa=-k,\ldots,+k$.

The spin tensors $\rho_{k\varkappa}(I_f)$ transform as an irreducible representation of the three-dimensional rotation group and are therefore irreducible tensors of rank k. The inverse relation

$$\rho_{I_f}(M_f,M_f')=(2I_f+1)^{-1/2}\sum_{k\varkappa}(-1)^{I_f-M_f}\times\langle I_fM_f'I_f-M_f|k\varkappa\rangle\rho_{k\varkappa}(I_f) \tag{5}$$

implies that the spin tensors of the density matrix are the coefficients of the expansion of the density matrix in a complete set of irreducible tensor operators. Equation (5) leads to an important property of the monopole spin tensor:

$$\mathrm{Tr}\,\rho_I(M_f,M_f')=\rho_{00}, \tag{6}$$

which for the normalization condition (2) is equal to unity.

Let us consider a binary nuclear reaction $a(I_a)+A(I_A)\rightarrow B^*(I_f)+b(I_b)$, with an excited nucleus B^* and a particle b formed in the final state. For this reaction the relation between the spin density matrices of the system before the collision ρ_i and after the collision ρ_f is determined, like that between the initial and final wave functions of the system, using the operator amplitude of the reaction or the operator T_{if} for the transition of the initial system $a+A$ in the state $|i\rangle$ to the final system $b+B^*$ in the state $|f\rangle$:

$$\rho_f=\langle T_{if}\rho_iT_{if}^+\rangle. \tag{7}$$

In the initial state the nuclei are independent, and so the density matrix of the system before the collision ρ_i factorizes into two pieces. In the density matrix of the final system we isolate the spin density matrix of the final nucleus B^* and average over the spin projections of the initial nuclei and the emitted particle. Then the spin density matrix of the nucleus B^* is given by

$$\rho_{I_f}(M_f,M_f',\Omega_b)=\sum_{M_aM_a'M_AM_A'M_bM_b'}\rho_{I_a}(M_a,M_a')\times\rho_{I_A}(M_A,M_A')T_{if,M_aM_AM_bM_f}(\Omega_b)\times T^*_{if,M_a'M_A'M_b'M_f'}(\Omega_b), \quad (8)$$

where $T_{ifM_aM_AM_bM_f}(\Omega_b)$ is the transition matrix element in the reaction $A(a,b)B^*$, M_a, M_A, and M_b are the spin projections of the nuclei a, A, and b, and $\rho_{I_a}(M_a,M_a')$ and $\rho_{I_A}(M_A,M_A')$ are the spin density matrices of the incident particles and the nuclear target.

If the density matrices of the incident particle $\rho_{I_a}(M_a,M_a')$ and the target nucleus $\rho_{I_A}(M_A,M_A')$ satisfy the normalization condition (2), the density matrix (8) is normalized to the differential cross section:

$$\mathrm{Tr}\,\rho_{I_f}(M_f,M_f',\Omega_b)=\frac{d\sigma}{d\Omega}. \quad (9)$$

Since in the case of unpolarized incident particles and targets the spin density matrices of the initial nuclei are diagonal, according to (3), in this case the spin density matrix of the nucleus B^* in the state with spin I_f and projection M_f is defined as

$$\rho_{I_f}(M_f,M_f',\Omega_b)=\frac{1}{(2I_a+1)(2I_A+1)}\times\sum_{M_aM_AM_bM_b'}T_{if,M_aM_AM_bM_f}(\Omega_b)\times T^*_{if,M_aM_AM_b'M_f'}(\Omega_b). \quad (10)$$

It follows from Eqs. (8) and (10) that the spin density matrix of the nucleus B^* produced in the nuclear reaction contains information not only about the spin state of this nucleus, but also about the entire nuclear reaction as a whole. In general, by using the density matrix it is possible to obtain the expectation value of any physical observable and to calculate the various characteristics of a nuclear reaction. The differential cross section of a reaction, which is what is studied traditionally and involves averaging over the spin projections of all the nuclei participating in the reaction, represents only one, the first, element of the spin tensors of the density matrix. The elements of the spin tensors of the density matrix different from ρ_{00} are not simply additional angular distributions; they are qualitatively new reaction characteristics. They are determined by the incoherent addition of reaction amplitudes depending on the spins and spin projections, and include the phase dependences of the amplitudes and their interference, and so are more sensitive to the reaction mechanism and the nuclear structure than are the differential cross sections. It is therefore important to study experimentally the spin tensors of the density matrix and to interpret them theoretically using various nuclear reaction models. In the following sections we shall discuss methods of experimentally and theoretically determining the components of the spin tensors of the density matrix in nuclear reactions.

3. METHODS OF CALCULATING THE PARTICLE–PARTICLE ANGULAR CORRELATION FUNCTIONS

Information about the properties of oriented systems produced in nuclear reactions and about the spin tensors of the density matrix of an excited nucleus can be obtained by studying the angular correlation functions of the reaction products. Here the nuclear reaction itself plays a dual role: on the one hand, it can act as the polarizer of the final particles and nuclei, and, on the other, it can act as the analyzer of the polarization of the incident particles.

The general formalism for calculating the angular correlation functions (ACFs) and the polarization[4] has been used to analyze various reactions. In reactions involving light particles, specific theoretical models of the angular correlations have been developed for the quasielastic knockout mechanism,[8,9] in the model of compound-nucleus formation,[27] and in the distorted-wave method.[28] The general formalism for calculating the ACFs has begun to be used for analyzing nuclear reactions involving complex particles and semiheavy ions (^{6,7}Li, ^{12}C, ^{14}N, and so on), α-transfer reactions, and multinucleon exchange reactions as theoretical models and methods for calculating the matrix element of the transition operator in such reactions have been developed.[29,30]

Another aspect of studying angular correlations is the experimental techniques for the direct reconstruction of the components of the spin tensors of the density matrix or the polarization tensors from the data on angular correlations. It is well known that this requires that the number of parameters of the ACFs be at least equal to the number of reconstructed components of the spin tensor; in particular, measurements of the ACFs in several radiation emission planes relative to the reaction plane are needed. A detailed discussion of this problem can be found in Ref. 6, where a method proposed by the authors for reconstructing the complete spin density matrix of an excited nucleus based on measurement of the particle–γ angular correlation function in various γ detection planes is justifed. Experimental techniques for reconstructing the polarization tensors of excited states of light nuclei in measurements of the particle–particle angular correlation function in reactions involving light particles have recently been developed in several laboratories abroad.[22,23] In these cases it is possible to perform a direct theoretical analysis of the experimental angular dependences of the spin tensors in various nuclear reaction models.

Let us consider the two-stage nuclear reaction $a(I_a)+A(I_A)\rightarrow B^*(I_f)+b(I_b)$, $B^*(I_f)\rightarrow C^*(I_0)+c(I_2)$, and define the angular correlation function $W(\Omega_b,\Omega_c)$ as the probability for the simultaneous detection of particle b in the direction Ω_b and the emission of particle c in the direction Ω_c. According to the general formalism,[4] the angular correlation function $W(\Omega_b,\Omega_c)$ is defined as the probability that the final system $B^*(I_f)\rightarrow C^*(I_0)+c(I_2)$ with density matrix ρ_{I_f} will be recorded by an ideal detector characterized by efficiency matrix $\varepsilon_{I_f}(\Omega_C,\Omega_c)$:

$$W(\Omega_b,\Omega_c)=\mathrm{Tr}(\rho_{I_f},\varepsilon). \quad (11)$$

The ideal detector must satisfy the following requirements:

1. The sensitivity of the detector to any particular characteristic of the recorded particle does not depend on the sensitivity to another characteristic.

2. The detector efficiency is independent of the particle energy.

3. The detector records particles c moving in a strictly defined direction.

Let us introduce spin efficiency tensors analogous to the spin tensors of the density matrix:

$$\varepsilon_{k\varkappa}(I_f)=(2I_f+1)^{-1}\sum_{M_fM_f'}(-1)^{I_f-M_f'}\langle I_fM_f'I_f -M_f|k\varkappa\rangle\varepsilon_{I_f}(M_f,M_f'). \tag{12}$$

Using Eqs. (5), (11), and (12), the angular correlation function $W(\Omega_b,\Omega_c)$ can be written as[4]

$$W(\Omega_b,\Omega_c)=\sum_{k\varkappa}\rho_{k\varkappa}(I_f)\varepsilon^*_{k\varkappa}(I_f). \tag{13}$$

Detailed descriptions of the methods of calculating the detector efficiency matrix and its spin tensors can be found in the literature.[5,24] Here we shall briefly mention only the main features and give the specific form of the spin efficiency tensors in the case of the emission of a particle possessing spin.

The efficiency matrix of an ideal detector describes the system $C(I_0)+c(I_2)$ produced as a result of the decay of a nucleus B^* in an excited state I_f^*. The decaying system can be characterized by the following angular-momentum addition scheme:

$$\mathbf{I}_f=\mathbf{I}_0+\mathbf{I}_2+\mathbf{L}=\mathbf{S}+\mathbf{L}, \tag{14}$$

where L is the orbital angular momentum of the relative motion of the decay products, and S is the channel spin. According to the definition of an ideal detector in Sec. 1, the efficiency tensor for recording the final system can be factorized into two components containing the spin and spatial efficiency tensors. The spin efficiency tensors can, in turn, be factorized into the efficiency tensors for recording the residual nucleus C and the radiation c:

$$\varepsilon_{k\varkappa}(I_0I_2(S)L{:}I_f;I_0I_2(S')L'{:}I_f) =\sum_{k_S\varkappa_Sk_L\varkappa_L}\varepsilon_{k_S\varkappa_S}(S,S')\varepsilon_{k_L\varkappa_L}(L,L')\langle k_S\varkappa_Sk_L\varkappa_L|k\varkappa\rangle \times\begin{pmatrix}S & L & I_f\\ S' & L' & I_f\\ k_S & k_L & k\end{pmatrix}, \tag{15}$$

where

$$\varepsilon_{k_S\varkappa_S}I_0I_2(S){:}I_0I_2(S')=\sum_{k_0\varkappa_0k_2\varkappa_2}\varepsilon_{k_0\varkappa_0}(I_0,I_0)\times\varepsilon_{k_2\varkappa_2}(I_2,I_2)\times\langle k_0\varkappa_0k_2\varkappa_2|k_S\varkappa_S\rangle \times\begin{pmatrix}I_0 & I_2 & S\\ I_0 & I_2 & S'\\ k_0 & k_2 & k_S\end{pmatrix}.$$

The spatial part of the efficiency matrix can be expressed in terms of angular-momentum eigenfunctions:

$$\varepsilon(Lm_L,L'm_L')=Y^*_{Lm_L}(\Omega_c)Y_{L'm_L'}(\Omega_c).$$

Accordingly, for the spatial tensor or the angular efficiency we obtain the expression

$$\varepsilon_{k_L\varkappa_L}(L,L')=D^{k_L}_{\varkappa_L0}(\Omega_c)C_{k_L0}(L,L'), \tag{16}$$

where

$$D^{k_L}_{\varkappa_L0}(\Omega_c)=(4\pi/(2k+1))^{1/2}Y^*_{k_L\varkappa_L}(\Omega_c)$$

are the matrices of finite rotations, and

$$C_{k_L0}(L,L')=(-1)^{L'}\frac{\sqrt{(2L+1)(2L'+1)}}{4\pi}\langle L0L'0;k_L0\rangle$$

are the parameters of the angular efficiency of detecting the radiation.

When the spin states of the residual nucleus C and the radiation are not fixed, their spin efficiency tensors are

$$\varepsilon_{k_0\varkappa_0}(I_0,I_0)=(2I_0+1)\delta_{k_00}\delta_{\varkappa_00},$$

$$\varepsilon_{k_2\varkappa_2}(I_2,I_2)=(2I_2+1)\delta_{k_20}\delta_{\varkappa_20}.$$

In this simple case the efficiency tensor (15) takes the form

$$\varepsilon_{k\varkappa}(I_f)=(2I_f+1)\sum_{SLL'}(-1)^{I_f+S}\sqrt{\frac{(2L+1)(2L'+1)}{(2k+1)(2I_2+1)}} \times\langle L0L'0|k0\rangle W(LI_fL'I_f{:}Sk)Y^*_{k\varkappa}(\Omega_c). \tag{17}$$

Let us also give a special case of Eq. (17), when the spin I_2 of particle c is zero, and the nucleus C is produced in the ground state with spin $I_0=0$. These conditions are satisfied in the decay of excited α-cluster nuclear states into an α particle and a residual nucleus in the ground state. Then $\varepsilon_{k\varkappa}$ takes the form

$$\varepsilon_{k\varkappa}(I_f)=(-1)^{I_f}(2I_f+1)(4\pi(2k+1))^{-1/2}\langle I_f0I_f0|k0\rangle Y^*_{k\varkappa}(\Omega_c). \tag{18}$$

If the spin tensors of the efficiency matrix are expressed as (17), the angular correlation function (13) takes the form

$$W(\Omega_b,\Omega_c)=\frac{\sqrt{2I_f+1}}{(2I_a+1)(2I_A+1)} \times\sum_{M_fM_f'}(-1)^{I_f}Y^*_{I_fM_f}(\Omega_b)Y_{I_fM_f}(\Omega_c) \times\sum_{M_aM_AM_b}|T_{if}|^2. \tag{19}$$

In more general cases the ACFs must be calculated from Eq. (13), using the specific expressions for the spin tensors of the density matrix and the spin efficiency.

Therefore, the theoretical interpretation of the ACFs depends on the physical model used to obtain the expression for the transition matrix element T_{if}.

Next we shall consider methods of calculating the angular correlation functions and the spin tensors of the density matrix in two complementary nuclear reaction models: the distorted-wave method with finite interaction range (EFR DWBA) and the modified model of compound-nucleus formation.

4. METHODS OF THEORETICALLY ANALYZING THE SPIN TENSORS OF THE DENSITY MATRIX

4.1. Formalism for calculating the spin tensors of the density matrix using the distorted-wave method with finite interaction range

The main features of this method are described in Refs. 31 and 32. Its three- and four-body approximations taking into account the cluster spectroscopy of light nuclei are discussed in Refs. 33 and 34.

In the distorted-wave method with finite interaction range (EFR DWBA) the matrix element of the transition operator between the initial and final states of the reaction is given by

$$M_{if}=\int\int d\mathbf{r}_a d\mathbf{r}_b \chi^{(-)}(\mathbf{k}_b\mathbf{r}_b)\langle\Psi_B\Psi_b|\mathbf{V}|\Psi_A\Psi_a\rangle\chi^{(+)}(\mathbf{k}_a\mathbf{r}_a), \tag{20}$$

where $\chi^{-}(\mathbf{kr})$ are the distorted waves in the entrance and exit reaction channels, and Ψ_B, Ψ_b, Ψ_A, and Ψ_a are the internal wave functions of the corresponding nuclei.

In the EFR DWBA the matrix element (20) of the nuclear reaction $A(a,b)B^*$ is written in the three-body approximation. Therefore, the reaction mechanism is determined by the splitting of the nuclear system into clusters with their spatial locations taken into account. Accordingly, we shall refer to mechanisms associated with dissociation of the incident particle $a\to b+x(B\to A+x)$ as direct processes, and mechanisms associated with dissociation of the target nucleus $A\to b+X(B\to a+X)$ as exchange processes. Since in the three-body approximation direct and exchange processes correspond to different cluster splittings, their matrix elements must be added incoherently, and the replacement of A by a and the angle θ_b in the center-of-mass frame by the angle $\pi-\theta_b$ must be formally distinguished.

In the matrix element (20) the potential $\mathbf{V}$ contains two terms. For direct processes it is the sum of the interaction potential of the clusters x and b in the incident particle a (the cluster stripping or pickup mechanism) and the potential for the virtual scattering of particle b on the nucleus A (the heavy-substitution mechanism). For exchange processes it is the sum of the interaction potential of the clusters b and X in the initial nucleus A (the heavy-stripping or heavy-pickup mechanism) and the potential for the virtual scattering of particles a and b (the substitution mechanism).

To calculate the matrix element for exchange processes, we shall use the following angular-momentum addition rules:

$$\vec{I}=\vec{\Lambda}_1+\vec{\Lambda}_2,\quad \vec{I}_1=\vec{\Lambda}_1+\vec{I}_X,\quad \vec{I}_2=\vec{\Lambda}_2+\vec{I}_X, \tag{21}$$

where l is the transferred angular momentum, Λ_1 and Λ_2 are the orbital angular momenta, and I_1 and I_2 are the total angular momenta of the relative motion of the nuclei $a+X$ in the final nucleus B and $b+X$ in the target nucleus A.

Finally, we write the matrix element of the reaction $A(a,b)B$ in the EFR DWBA for exchange proceses as

$$\begin{aligned}T_{if}(\Omega_b)=&\sum_{I_1M_1I_2M_2}\langle I_aM_aI_1M_1|I_fM_f\rangle\\&\times\langle I_bM_bI_2M_2|I_AM_A\rangle((2I_1+1)(2I_2+1))^{1/2}\\&\times\sum_{lm_l} i^{l+M_2}\langle I_2-M_2I_1M_1|lm_l\rangle\\&\times\sum_{\Lambda_1\Lambda_2I_XE_X}(-1)^{\Lambda_1+\Lambda_2}\\&\times\theta_{l\Lambda_1\Lambda_2I_1I_2I_X}\cdot\beta_{lm_l\Lambda_1\Lambda_2I_XE_X}(\Omega_b).\end{aligned} \tag{22}$$

Here $\theta_{l\Lambda_1\Lambda_2I_1I_2I_XE_X}$ is the structure factor,[5,33] containing information about the reduced widths $\theta^{B\to a+X}_{\Lambda_1I_1I_X}$ and $\theta^{A\to b+X}_{\Lambda_2I_2I_X}$ of the decay of the nuclei B and A via the channels $a+X$ and $b+X$, respectively. The kinematical factors $\beta_{lm_l\Lambda_1\Lambda_2I_XE_X}(\Omega_b)$ are the overlap integrals of the incoming and outgoing "distorted" waves, the wave functions of the relative motion, and the interaction potential, and contain essential information about the reaction mechanism.

Combining Eqs. (4), (10), and (22), for the spin tensors of the density matrix of the nucleus in the state I_f in the EFR DWBA we obtain

$$\begin{aligned}\rho_{k\varkappa}(\theta_b)=&\frac{2I_f+1}{2I_a+1}\frac{1}{E_aE_b}\frac{k_b}{k_a}\\&\times\sum_{I_1I_1'I_2}(-1)^{I_f+I_2+I_a}w(I_1I_fI_1'I_f:I_ak)((2I_1+1)\\&\times(2I_1'+1))^{1/2}\sum_{ll'm_lm_l'}(-1)^{l+l'+m_l'}\\&\times\langle lm_ll_1-m_{l'}|k\varkappa\rangle w(lI_1l'I_1':I_2k)((2l+1)\\&\times(2l'+1))^{1/2}\sum_{\substack{\Lambda_1\Lambda_2I_XE_X\\ \Lambda_1'\Lambda_2'I_X'E_X'}}\theta_{l\Lambda_1\Lambda_2I_1I_2I_X}\theta_{l'\Lambda_1'\Lambda_2'I_1'I_2'I_X'}\\&\times\beta_{lm_l\Lambda_1\Lambda_2I_XE_X}(\Omega_b)\beta^*_{l'm_l'\Lambda_1'\Lambda_2'I_X'E_X'}(\Omega_b).\end{aligned} \tag{23}$$

In the special case considered above, where the excited level of the nucleus B^* decays with the emission of an α particle, the angular correlation function (19) in the EFR DWBA for the direct α-transfer mechanism (cluster stripping) takes the form

$$W(\Omega_b,\Omega_c)=\frac{\sqrt{2I_f+1}}{(2I_A+1)}\sum_{I_2M_2M_A}\left|\sum_{M_f}M_{I_fI_2M_2M_AM_f}\times(\Omega_b)Y_{I_fM_f}(\Omega_c)\right|^2, \quad (24)$$

where

$$M_{I_fI_2M_2M_AM_f}(\Omega_b)=\sum_{I_1M_1}\langle I_AM_AI_1M_1|I_fM_f\rangle\times(2I_1+1)^{-1/2}(2I_A+1)^{-1/2}\times\sum_{lm_l}i^l\langle I_2-M_2I_1M_1|lm_1\rangle\times\sum_{\Lambda_1\Lambda_2}(-1)^{l+\Lambda_1+\Lambda_2}\theta_{l\Lambda_1\Lambda_2I_1I_2I_x}\times\beta_{lm_l\Lambda_1\Lambda_2I_xE_x}(\Omega_b).$$

The EFR DWBA has been realized computationally in a number of codes[41,57–61,85] which can be used to calculate the differential cross sections of one- and multinucleon transfer reactions. Let us briefly discuss the OLYMP-5 code (Ref. 41). This code, which realizes the EFR DWBA most systematically, allows the calculation of not only the differential cross sections of multinucleon transfer reactions, but also the spin tensors of the density matrix and the polarization tensors of the excited nucleus, the angular correlation functions, and the populations of the magnetic sublevels of excited states of the final nucleus. The reaction matrix element includes all four single-stage reaction mechanisms pertaining to direct and exchange processes. According to Eq. (22), in the matrix element for exchange processes it is possible to sum coherently over the different angular momenta Λ_1 and Λ_2 of the relative motion, which corresponds to the inclusion of excited states of the intermediate nucleus.

The OLYMP-5 code can be used to analyze reactions involving semiheavy ions in which high-lying quasistationary states are formed. Therefore, the numerical procedure for finding the bound-state wave functions usually used in EFR DWBA codes is modified in the OLYMP-5 code. In Sec. 5.2 below we shall discuss a method of finding wave functions of the Gamow type describing quasistationary states with positive binding energy and nonzero decay width.

It is known that reactions induced by semiheavy ions with the formation of strongly excited high-lying states must be peripheral, since semiheavy ions of relatively low energy cannot penetrate deeply inside the nucleus. As noted above, the specific features of calculations in the EFR DWBA are associated with calculations of the kinematical factors $\beta_{lm_l\Lambda_1\Lambda_2I_XE_X}(\Omega_b)$ (Refs. 34 and 60). In particular, the kinematical factors contain sums, over the partial orbital angular momenta L_a and L_b of the entrance and exit channels, of double radial overlap integrals of partial distorted waves and nuclear form factors. The correct calculation of the radial integrals at the nuclear periphery reflecting the features of the interaction of semiheavy ions is ensured by the correct asymptote of the Gamow wave functions. However, in the interior of the nucleus for $r\to 0$ the rate of falloff of the wave functions of the relative motion of the clusters in the excited nucleus often does not correspond to the actual interaction process of semiheavy ions. As a result, when a numerical procedure is used to find the wave functions of quasibound states, the contribution of the interior of the nucleus to the radial integral can be overestimated. One way to correct this in EFR DWBA calculations is to cut off the sum over the partial orbital angular momenta L_a and L_b in the entrance and exit channels at small L, i.e., to introduce a parameter $L_{\min}$. As will be shown below when we discuss the actual results, the use of a cutoff in L leads to agreement between the calculations and the experimental data not only when studying the interaction of the semiheavy ions ^{12}C and ^{14}N, but also when studying the polarization tensor of the light nucleus ^{6}Li.

4.2. The formalism of calculating the spin tensors of the density matrix in the modified compound-nucleus model

The model of a nuclear reaction occurring via the stage of compound-nucleus formation is based on the idea that the two processes, formation and decay of the compound nucleus, are independent of each other. It is assumed that the incident particle energy is distributed according to the laws of statistical mechanics over all the nuclear degrees of freedom, i.e., that thermodynamical equilibrium is established in the system. When the reaction is induced by particles of sufficiently high energy, the excited levels of the compound nucleus will lie in the continuum. The features of reactions occurring with the formation of a compound nucleus in the continuum are to a large extent determined by the fact that the compound nucleus decays in a very large number of different ways. The statistical theory first developed in Refs. 35–37, called the Hauser–Feshbach formalism, successfully describes the cross sections for such reactions, which are characterized by a smooth, nonresonance energy dependence.

The calculation of the cross section for the reaction $A(a,b)B$ in the approximation of the statistical model reduces to the calculation of the transmission coefficients T_{ll}^{Ic} of the various channels, defined as the ratio of the number of particles passing through the nuclear barrier into the interior of the nucleus to the number of incident particles.

The scheme for calculating reaction cross sections in the Hauser–Feshbach formalism has been realized in a number of computer codes such as STATIC (Ref. 38) and HELGA (Ref. 39). In these codes the transmission coefficients T_{ll}^{Ic} are calculated in the optical model neglecting the spin–orbit interaction, using the S matrix of elastic scattering. The decay probability of the compound nucleus must include all possible open channels. Calculations of this quantity usually include a limited number of the most important decay channels (for example, up to 10 channels in the HELGA code), and also the contribution of the continuum of the residual nuclei, which is calculated using the expressions for the level density in various models.

The authors of Ref. 40 proposed a version of the standard compound-nucleus model modernized in the following ways: direct inclusion of the structure of the nuclei participating in the reaction, and inclusion of the heavy-stripping mechanism (direct transfer of a heavy cluster from the target nucleus to the incident particle) in calculating the transmission coeffficients T_l and the spin–orbit interaction.

Let us review the derivation of the expressions for the spin tensors of the density matrix in the modified statistical model of the compound nucleus.

Using the fact that the reaction mechanism involving compound-nucleus formation presupposes that the formation and decay of the compound nucleus are independent processes, we write the reaction matrix element as the product of two factors, one corresponding to the formation of a quasistationary state of the compound nucleus with spin I_C, and the other corresponding to its decay:

$$M_{if}=\langle\psi_f|\psi_C\rangle\langle\psi_C|\psi_i\rangle, \tag{25}$$

where ψ_i, ψ_f, and ψ_C are the wave functions of the initial, final, and intermediate quasistationary states.

We define the following angular-momentum addition rules in the channel-spin representation:

$$\vec{I}_1=\vec{I}_a+\vec{I}_A, \quad \vec{I}_2=\vec{I}_b+\vec{I}_B, \quad \vec{I}_C=\vec{I}_1+\vec{l}_a=\vec{I}_2+\vec{l}_b,$$

where l_a and l_b are the orbital angular momenta of the particle relative motion in the entrance and exit channels, and I_1 and I_2 are the spins of the entrance and exit channels.

In this representation the wave functions take the form

$$\Psi_i=\Psi_A(\mathbf{g}_A)\cdot\Psi_a(\mathbf{g}_a)\cdot\chi(\mathbf{k}_a,\mathbf{r}_a),$$

$$\Psi_f=\Psi_B(\mathbf{g}_B)\cdot\Psi_b(\mathbf{g}_b)\cdot\chi(\mathbf{k}_b,\mathbf{r}_b), \tag{26}$$

$$\Psi_C=\sum_{I_1M_1I_CM_C}\langle I_aM_aI_AM_A|I_1M_1\rangle$$

$$\times\langle I_1M_1l_am_a|I_CM_C\rangle\theta_{l_aS_aI_a}\cdot\psi_A(\mathbf{g}_A)\psi_a(\mathbf{g}_a)\phi_{la}(\mathbf{r}_a)$$

$$=\sum_{I_2M_2I_CM_C}\langle I_bM_bI_BM_B|I_2M_2\rangle\langle I_2M_2l_bm_b|I_CM_C\rangle$$

$$\times\theta_{l_bS_bI_b}\cdot\psi_B(\mathbf{g}_B)\psi_b(\mathbf{g}_b)\phi_{lb}(\mathbf{r}_b).$$

These nuclear wave functions depend on the internal variables $\mathbf{g}_i$; $\chi(\mathbf{k}_a,\mathbf{r}_a)$ and $\chi(\mathbf{k}_b,\mathbf{r}_b)$ are the wave functions of the relative motion (distorted waves) in the entrance and exit reaction channels, $\phi_{la}(\mathbf{r}_a)$ and $\phi_{lb}(\mathbf{r}_b)$ are the wave functions of the relative motion of the clusters in the bound state, and $\theta_{l_aI_aI_1}$ and $\theta_{l_bI_bI_1}$ are the amplitudes of the reduced width of the decay of the compound nucleus via the channels $A+a$ and $B+b$.

Using the definition of the partial decay widths of a quasistationary state and the expressions for expanding the distorted waves in partial waves, let us calculate the integral over the internal variables in the matrix element (25). This gives the matrix element (25) in the form

$$M_{if}=\sum_{\substack{I_1M_1I_2M_2I_CM_C\\ l_am_al_bm_b}}\langle I_bM_bI_BM_B|I_2M_2\rangle$$

$$\times\langle I_2M_2l_bm_b|I_CM_C\rangle\langle I_aM_aI_AM_A|I_1M_1\rangle$$

$$\times\langle I_1M_1l_am_a|I_CM_C\rangle\gamma_{l_bI_b}^{C\to B+b}\gamma_{l_aI_a}^{C\to A+a}$$

$$\times Y_{l_bm_b}(\theta_{k_b},\varphi_{k_b})Y^*_{l_am_a}(\theta_{k_a},\varphi_{k_a}). \tag{27}$$

We choose a coordinate system such that the z axis points along the incident particle momentum and $\varphi_b=0$.

Combining Eqs. (4), (10), and (27) and performing the necessary algebra, we obtain the following expression for the density matrix:

$$\rho_{I_f}(M_f,M_f')$$

$$=\frac{1}{2k_a^2(2I_a+1)(2I_A+1)}\sum_{k\varkappa}\langle I_BM_BI_B-M_B|k\varkappa\rangle$$

$$\times\sum_{\substack{I_1I_2I_CI_2'l_bl_al_b'l_a'\\ lm_ll'm_l'}}(2I_C+1)^2$$

$$\times\sqrt{(2I_2+1)(2I_2'+1)(2l+1)(2l'+1)(2l_a+1)(2l_a'+1)}$$

$$\times(-1)^{2I_C+I_B-I_1+I_B}\langle l_a0l_bm_b|lm_l\rangle\langle l_a'0l_b'm_b'|l'm_l'\rangle$$

$$\times\langle l'm_l'l'-m_l|k\varkappa\rangle w(I_1l_aI_2l_b;I_Cl)\cdot w(I_1l_a'I_2'l_b';I_Cl)$$

$$\times w(I_BI_2I_BI_2';I_bk)w(I_2lI_2'l';I_1k)Y_{l_bm_b}(\theta_{k_b},0)$$

$$\times Y^*_{l_b'm_b'}(\theta_{k_b},0)(\gamma_{l_bI_bI_2}^{C\to B+b})^2\cdot(\gamma_{l_aI_aI_1}^{C\to A+a})^2. \tag{28}$$

The density matrix $\rho_{I_f}(M_f,M_f')$ in (28) is determined by only a single resonance. In the region of the quasicontinuous spectrum, where resonances overlap strongly, it is necessary to average the contribution of each and sum over all the resonances in the averaging interval.

Since we are considering quasistationary states λ of a compound nucleus, which satisfy an exponential decay law, the density matrix $\bar{\rho}_{If}(M_f,M_f')$ averaged over the energy distribution is described by the expression

$$\overline{\rho_{I_f}}(M_f,M_f')=\frac{1}{\Delta E}\int_{E-\Delta E/2}^{E+\Delta E/2}\frac{\rho_{I_f}(M_f,M_f')}{(E-E_\lambda)^2+\frac{1}{4}\Lambda_\lambda^2}\,dE', \tag{29}$$

where E_λ is the energy of the level λ, Γ_λ is the total width of the level λ, and E is the incident particle energy.

After summing over all the resonances in the averaging interval, we arrive at the transmission coefficients $T_{ll}^{I_C}$, which are related to the average partial width $\Gamma_{ll}^{I_C}$ and the average spacing between levels D_{I_C} as

$$T_{ll}^{I_C}=2\pi\frac{\Gamma_{ll}^{I_C}}{D_{I_C}}.$$

Finally, the spin tensors of the density matrix in the statistical limit of the compound-nucleus model have the form

$$\rho_{k\varkappa}(\theta_b)=\frac{1}{2K_a^2}\frac{\sqrt{I_f+1}}{(2I_a+1)(2I_A+1)}$$
$$\times\sum_{I_1I_2I_CI_2'}(-1)^{2I_C+I_f-I_b}(2I_c+1)^2$$
$$\times\sqrt{(2I_2+1)(2I_2'+1)}w(I_fI_2I_fI_1';I_bk)$$
$$\times\sum_{lm_ll'm_l'l_al_a'l_bl_b'}$$
$$\times\sqrt{(2l+1)(2l'+1)(2l_a+1)(2l_a'+1)}$$
$$\times\langle l_a0l_bm_b|lm_l\rangle\cdot\langle l_a'0l_b'm_b'|l'm_l'\rangle$$
$$\times\langle lm_ll'm_l'|k\varkappa\rangle w(I_1l_aI_2l_b;I_Cl)w(I_1l_a'I_2'l_b';I_Cl')$$
$$\times w(I_2l_2I_1'l';I_1k)\frac{T^{I_C}_{l_aI_1l_a'I_1}\cdot T^{I_C}_{l_bI_2l_b'I_2'}}{g(I_C)}$$
$$\times P_{l_bm_l}(\theta_b)P_{l_b'm_l'}(\theta_b), \qquad (30)$$

where $P_{l_bm_l}(\theta_b)$ are the associated Legendre polynomials.

The denominator in (30) is referred to as the total decay width of the compound nucleus and includes all the energetically allowed decay channels of the compound nucleus:

$$g(I_C)=\sum_n\sum_{l_2}\sum_{I_2=|l_2-I_C|}^{l_2+I_C}\sum_{I_f=|I_2-I_b|}^{I_2+I_b}\left\{\sum_{E_f=0}^{E_C}T^{I_C}_{l_2I_2}+\int_{E_C}^{E_f^*}T^{I_C}_{l_2I_2}\rho(E_f^*,I_f)dE_f^*\right\}, \qquad (31)$$

where n is the number of open channels, E_f^* is the energy of the excited level of the residual nucleus B, and E_C is the energy at the bottom of the continuum (the edge of the continuum).

We have written an original computer code CNCOR to calculate the spin tensors of the density matrix, the populations of the magnetic sublevels, the angular correlation functions, and the differential cross sections in the modified statistical model of the compound nucleus as applied to reactions involving semiheavy ions.[41] The most important problems in realizing this program were the calculation of the transmission coefficients $T_{lI}^{I_C}$ and the total decay width $g(I_C)$.

The transmission coefficients $T_{lI}^{I_C}$ can be expressed in terms of the elements of the scattering matrix in the entrance and exit channels as

$$T_{lI}^{I_C}=1-|S_{lI}^{I_C}|^2. \qquad (32)$$

In the CNCOR code the S-matrix elements are found in the optical model by solving the Schrödinger equation with the corresponding complex spin–orbit potential.

The nuclear spin–orbit potential including noncentral interactions has the form

$$V_{lI}(r)=\left(\frac{\hbar}{m_\pi c}\right)\left[-\frac{1}{r}\frac{df_4}{dr}V_{lI}-i\frac{1}{r}\frac{df_5}{dr}W_{lI}\right], \qquad (33)$$

where $\hbar/m_\pi c$ is the Compton wavelength of the pion, and V_{lI} and W_{lI} are the depths of the real and imaginary parts of the spin–orbit potential. The radial dependences f_4 and f_5 are chosen in the standard Woods–Saxon form. The details of the calculation of the coefficients $T_{lI}^{I_C}$ can be found in Refs. 42 and 43.

The calculation of the total decay width $g(I_C)$ requires knowledge of the energy, spin, and parity of all the states of the residual nucleus in all the decay channels. A compound nucleus with spin I_C decaying via a certain channel can produce a nucleus whose excited levels lie both in the discrete spectrum and in the continuum. The first term in (31) takes into account the fraction due to levels in the discrete spectrum. It is easy to include this fraction after summing the transmission coefficients over the energies of all the low-lying discrete levels up to the energy E_C, the edge of the continuum. The second term in (31) determines the total contribution of all the continuum levels to the total decay width. When integrating over the entire energy range of the continuum it is necessary to include the nonuniformity of the level distribution in the energy range by introducing the level density of the final nucleus $\rho(E_B^*,I_B)$. The integration in the second term of (31) runs from the energy E_C to E_B^*, the maximum allowed excitation energy of the final nucleus, defined as

$$E_B^{*\max}=E_{\text{lab}}\frac{m_a}{m_a+m_A}+Q,$$

where E_{lab} is the energy of the incident particle in the lab frame, m_a and m_A are the masses of the incident particle a and the target nucleus A, and Q is the heat of the reaction.

The value of E_C, the edge of the continuum, can be determined from the appearance of a small probability for particle emission, using tabulated experimental data on the structure of the spectra and the decay of excited nuclear levels; see, for example, Ref. 44.

The integration of the coefficients T in the continuum is performed using specific expressions for the nuclear level density. In the CNCOR code we use a model in which the nucleus is treated as a degenerate Fermi gas. In this case the level density of a nucleus with excitation energy E^* and spin I has the form[45]

$$\rho(E^*,I)=(2I+1)\cdot\exp\left[-\left(I+\frac{1}{2}\right)^2\Big/2\sigma^2\right]\rho(E^*), \qquad (34)$$

where

$$\rho(E^*)=\frac{\exp(2\sqrt{aU})}{12a^{1/4}(U)^{5/4}(2\sigma^2)^{3/2}}.$$

The level density is determined by the effective excitation energy and two model parameters: the level-density parameter a and the spin-dependence parameter σ^2. The effective energy U is defined as

$$U=E^*-P(Z)-P(N),$$

where $P(Z)$ and $P(N)$ are the pairing energies of the proton and neutron components, which have been calculated using semiempirical atomic mass formulas and tabulated (see, for example, Ref. 46). The spin-dependence parameter is determined by the program from the expression

$$\sigma^2 = 0.1459\sqrt{aU}\cdot A^{2/3} \tag{35}$$

for nuclei with mass number A (Refs. 47 and 48). The value of the level-density parameter a is chosen on the basis of the expressions proposed by Gilbert and Cameron.[47,48]

The yrast-line cutoff in each open channel is determined from

$$E^{\text{yrast}}(I) = [I(I+1) - K^2]\,\frac{\hbar^2}{2F_s}, \tag{36}$$

where K is the spin of the ground state of the residual nucleus, $F_s = \frac{2}{5}mAR^2$ is the moment of inertia of a rigid sphere, $R = r_0 A^{1/3}$ F, m is the nucleon mass in MeV, and I^{yrast} denotes the angular momentum of a rigid, spherical rotating body at a given excitation energy E^{yrast} given by (36).

5. STUDY OF QUASISTATIONARY α-CLUSTER STATES OF NUCLEI IN REACTIONS INDUCED BY ^{6,7}Li IONS USING $d-\alpha$ AND $t-\alpha$ ANGULAR CORRELATIONS

5.1. Experimental study of the $d-\alpha$ and $t-\alpha$ angular correlation functions

Already 20 years ago, reactions involving the transfer of an α-particle induced by semiheavy ions proved to be a source of new information about the α-particle rotational states of nuclei of the $1p$ and $2s-1d$ shells.[49–51] Without dwelling in detail on the full set of results obtained for various types of α-transfer reactions, we shall give a general review of the literature[12,52] and a monograph devoted to the spectroscopic and cluster aspects of multinucleon transfer reactions.[53] We note that α-transfer reactions are directly related to cluster representations of the structure of light nuclei and the presence of excited quasistationary states of α-cluster nature in p- and sd-shell nuclei. Nuclear α-transfer reactions induced by lithium ions, (^{6}Li,d) and (^{7}Li,t), play a special role. It was for these ions that the exceptional selectivity in the population of the nuclear final states was first discovered experimentally[49–51] and later repeatedly confirmed. Experimental studies of the cross sections for these reactions, and also for α-transfer reactions induced by ^{16}O (Ref. 54) and ^{11}B, ^{12,13}C (Ref. 55) ion beams used later on, focused mainly on the discovery and study of the spectroscopic properties of excited cluster states. Theoretical analysis of the results became especially important, as it allowed comparison of the spectroscopic factors obtained experimentally with the theoretical predictions of a given reaction model. Analyses of this type were made possible by the development of a theoretical method and construction of the corresponding computer programs[57–61] based on the Born approximation with distorted waves and exactly including the potentials and sizes of the interaction region and recoil effects (the EFR DWBA).

Meanwhile, the study of transfer reactions coincided with the intense development of theoretical methods of constructing cluster wave functions of nuclei and calculating the cluster spectroscopic factors, such as the antisymmetrized cluster model,[62,63] the resonating-group method (RGM),[64] and methods of solving the problem of three or more bodies.[65–67]

Experimental studies of α-transfer reactions induced by ^{6,7}Li ions and the theoretical analysis of the excitation cross sections of a number of low-lying cluster states in ^{12}C, ^{16}O, ^{18}F, and ^{20}Ne using the EFR DWBA and the compound-nucleus model in the Hauser–Feshbach formalism were carried out in Refs. 68–72. Whereas spectroscopic factors in good agreement with each other and with the theoretical ones from the shell model and the cluster model were obtained for ^{20}Ne, it proved impossible to obtain consistent values for ^{16}O (Ref. 44).

The angular distributions of the emitted particles in cases where the final nucleus is formed in a highly excited state lose the features characteristic of direct reactions—the forward directivity and the oscillatory structure, and become uninformative. A method was proposed in Ref. 11 for measuring the double differential cross sections—the particle–particle angular correlation functions. Its emphasis is in a new direction which is more productive from the viewpoint of the spectroscopy of highly excited α-cluster states and study of the role of various reaction mechanisms involving light heavy ions.[13,73,74] Those authors showed that in the reaction ^{12}C(^{6}Li,d)^{16}O*(α)^{12}C, the $d-\alpha$ angular correlation measured in the reaction plane at small deuteron emission angles relative to the beam direction ($\theta_d = 10°$) can be approximated by a simple function:

$$W(\theta_d, \theta_\alpha) = \frac{2I_f+1}{4\pi}\,[P_{I_f}(\cos(\theta_\alpha - \theta_0))]^2, \tag{37}$$

where P_{I_f} is a Legendre polynomial, I_f is the spin of the excited state of ^{16}O, θ_α is the α-particle emission angle relative to the direction of the momentum of the ^{16}O nucleus in the rest frame of this nucleus, and θ_0 is the shift relative to this direction.

Measurement of the ACFs in the reaction (^{6}Li,d) led to the discovery and identification in spin and parity of new high-lying (with excitation energy E^* lying between 10 and 30 MeV) α-cluster states in ^{16}O (Ref. 11), ^{20}Ne (Ref. 75), ^{28}Si (Ref. 76), ^{18}O (Ref. 77), and ^{18}F (Ref. 78) nuclei.

The experimental study of particle–particle correlations in reactions induced by semiheavy ions is a very difficult undertaking requiring a large amount of time for accumulating sufficient statistics. Therefore, the measurements which have been carried out so far have been made in a single emission plane, which is insufficient for reconstructing the components of the spin tensors of the density matrix. Nevertheless, analysis of the angular correlation functions and the differential cross sections of the corresponding reactions gives interesting information both about the structure of low-lying cluster states, and about the dynamics and mechanisms of the reactions themselves.

When deuterons are recorded at small angles relative to the incident beam, the simple angular dependence of the ACFs observed at various energies of the ^{6}Li ions and for various nuclear states indicates a preferred population of one spin projection of the excited state of the final nucleus: $m_f = 0$. A characteristic feature of the $d-\alpha$ correlation functions is the small, state-dependent, shift of the symmetry axis of the ACF (37) by an angle θ_0 relative to the recoil direction of the final nucleus.

The interpretation of the reaction mechanism as the direct transfer of an α-particle cluster and the simple form of the ACF provided justification for the first calculations of the angular correlations using the DWBA for the stripping mechanism.[79] The calculations showed that the shift of the symmetry axis of the ACF (37) by the angle θ_0 relative to the direction of the momentum transfer in the plane-wave approximation can be attributed to distortions of the plane waves in the entrance and exit reaction channels. The $d-\alpha$ correlation functions for the 10.35-MeV (4^+) state produced in the reaction ^{12}C(^{6}Li,d)^{16}O*(α)^{12}C have been calculated within the EFR DWBA using the LOLA (Ref. 58) and CORELA (Ref. 80) codes. The exact inclusion of the plane-wave distortions and realistic potentials and wave functions made it possible to explain the observed shift of the ACF symmetry axis. It led to agreement with experiment and allowed study of the dependence of the shift θ_0 on many of the parameters of the calculation. The calculated shift of the first maximum of the ACF relative to the direction of the momentum transfer proved to be especially sensitive to changes of the parameters of the real part of the optical potential of the $d+^{16}$O interaction in the exit channel, and also to the parameters of the wave function of the $\alpha+^{12}$C relative motion in ^{16}O. The ACF calculations demonstrated the discrete and continuous ambiguities of the optical potentials known in elastic scattering. It should be emphasized that, in contrast to elastic scattering, analysis of the ACFs allows study of the parameters of the optical potentials of nuclei in excited states, and also selection of the parameters of the wave functions of the relative motion of the clusters in excited nuclear states.

However, the clear experimental picture that we have described, which has a simple theoretical interpretation, was spoiled by the observation of suppression of the first maximum in the $\alpha-d$ correlation function for the high-lying 20.9-MeV (7^-) level of ^{16}O in the reaction (^{6}Li,d) (Ref. 81). This fact stimulated extension of the studies of high-lying α-cluster states using both $d-\alpha$ and $t-\alpha$ correlations, and also more detailed theoretical analysis using the distorted-wave method with finite interaction range.

To better understand the dynamics of the reactions (^{6}Li,d) and (^{7}Li,t) in the distorted- and plane-wave approximations, we shall follow Ref. 82 and write the amplitude entering into (23) for the angular correlation function in the plane-wave approximation (PWA):

$$M^{\mathrm{PWA}}_{I_f I_2 M_2 M_A M_f}(\Omega_b)=\sum_{I_1 M_1}\langle I_A M_A I_1 M_1|I_f M_f\rangle \times(2I_f+1)^{1/2}(2I_A+1)^{-1/2} \times\sum_{lm_l}\langle I_2-M_2 I_1 M_1|lm_l\rangle \times\sum_{\Lambda_1\Lambda_2}(-1)^l\theta_{l\Lambda_1\Lambda_2 I_1 I_2 I_x}(2l+1)^{-1/2} \times\sum_{\mu_1\mu_2}(-1)^{\mu_2}\langle\Lambda_1\mu_1\Lambda_2-\mu_2|lm_l\rangle \times F_{\Lambda_1}(q)A_{\Lambda_2}(p)Y^*_{\Lambda_1\mu_1}(\hat{q})Y_{\Lambda_2\mu_2}(\hat{p}). \tag{38}$$

The amplitude (38) is written in terms of the nuclear form factors $F_{\Lambda_1}(q)$ and $A_{\Lambda_2}(p)$, depending on the momenta q and p:

$$\mathbf{q}=\mathbf{k}_x-\frac{A}{B}\mathbf{k}_y,\quad \mathbf{p}=\mathbf{k}_y-\frac{y}{x}\mathbf{k}_x. \tag{39}$$

Let us consider the case where the reaction occurs on nuclei with zero spin $I_A=0$, and the spin of the transferred particle x is $I_x=0$ (the case of direct α-particle transfer on the nuclei ^{12}C and ^{16}O). Owing to simplification of the expression for the structure factor $\theta_{l\Lambda_1\Lambda_2 I_1 I_2 I_x}$ (Ref. 82), the amplitude (38) takes the form

$$M^{\mathrm{PWA}}_{I_f\Lambda_2 M_2 M_f}(\Omega_b)=\sum_{lm_l}\langle\Lambda_2-M_2 I_f M_f|lm_l\rangle(2\Lambda_2+1)^{-1/2} \times\sum_{\mu_1\mu_2}(-1)^{l+\mu_2}\langle I_f\mu_1\Lambda_2-\mu_2|lm_l\rangle \times F_{I_f}(q)A_{\Lambda_2}(p)Y^*_{I_f\mu_1}(\hat{q})Y_{\Lambda_2\mu_2}(\hat{p}). \tag{40}$$

Therefore, if the final particle y is emitted in the direction of the incident beam, i.e., $\theta_y=0°$, then $\mu_1=\mu_2=0$, and accordingly $m_1=0$, $M_f=M_2$. Owing to the orthonormality of the Clebsch–Gordan coefficients, for the amplitude (40) we obtain

$$M^{\mathrm{PWA}}_{I_f\Lambda_2}(\theta_b=0°)=(-1)^{\Lambda_2}(2\Lambda_2+1)^{-1/2} \times F_{I_f}(q)A_{\Lambda_2}(p)\delta_{M_2 0}.$$

In this case the simplified expression for the angular correlation function (24) takes the form

$$W^{\mathrm{PWA}}(\theta_b=0°,\theta_\alpha)=N|P_{I_f}(\theta_\alpha)|^2,$$

$$N=\sum_{\Lambda_2}|T^{\mathrm{PWA}}_{l_f\Lambda_2}(\theta_b=0°)|^2, \tag{41}$$

i.e., it contains the square of the Legendre polynomial of order I_f and is independent of the angular momentum Λ_2 of the relative motion of the nuclei at the $a\to b+x$ vertex. This means that the ACFs for both the (^{6}Li,d) reaction and the (^{7}Li,t) reaction must be a polynomial in the plane-wave approximation at small deuteron or triton emission angles.

The experimental study of the $t-\alpha$ angular correlation functions in the reaction ^{12}C(^{7}Li,t)^{16}O*(α)^{12}C at $E_{\mathrm{Li}}=45$ MeV carried out in Ref. 83 showed that normal polynomial behavior of the ACFs is observed for the levels 20.9

MeV (7^-), 16.3 MeV (6^+), and 14.6 MeV (5^-). That is, the specific dynamics of direct α-transfer nuclear reactions is manifested in the $d-\alpha$ and $t-\alpha$ angular correlation functions in the reactions (^{6}Li,d) and (^{7}Li,t).

The effect of distortions of the plane waves on the form of the ACFs was also studied theoretically for (^{7}Li,t) reactions.[82,84] The first calculations of $W(\Omega_t,\Omega_\alpha)$ taking into account plane-wave distortions in the reaction ^{16}O(^{7}Li,t)^{20}Ne*(α)^{16}O at $E_{\rm Li}$=20 and 24 MeV for a series of excited states of the ^{20}Ne nucleus (from 3^- to 8^+; Ref. 84) showed that the effect of optical distorting potentials is so important that even for triton emission in the direction of the incident beam (θ_t=0°), and also at θ_t=180°, $W(\Omega_t,\Omega_\alpha)$ is deformed (it is observed that the maxima shift in angle and that their relative intensity is changed), and the calculated $t-\alpha$ correlation function does not have the form of squared Legendre polynomials.

In Ref. 82 we performed a theoretical study of the $t-\alpha$ angular correlation functions in the reactions ^{12}C(^{7}Li,t)^{16}O*(α)^{12}C and ^{16}O(^{7}Li,t)^{20}Ne*(α)^{16}O for various energies of the ^{7}Li ion and several excited α-cluster states of the ^{16}O and ^{20}Ne nuclei within the EFR DWBA using the OLYMP-5 (Ref. 85) and CORELA (Ref. 80) codes. The calculations confirmed the conclusion that the distorting potentials strongly affect the form of the $t-\alpha$ correlation function in (^{7}Li,t) reactions, and also revealed that $W(\Omega_t,\Omega_\alpha)$ depends on the ^{7}Li energy. As in the reaction ^{12}C(^{7}Li,t)^{16}O*(α)^{12}C for the level 14.6 MeV ($I_f=5^-$) at $E_{\rm Li}$=35 MeV, the inclusion of the optical potential for the interaction of the emitted triton with the ^{16}O nucleus leads to suppression of the principal maximum of $W(\Omega_t,\Omega_\alpha)$, which appears only when the nuclear interaction is completely switched off. A similar result was also obtained for the reaction ^{16}O(^{7}Li,t)^{20}Ne*(α)^{16}O at $E_{\rm Li}$=24 MeV for the level 10.26 MeV ($I_f=5^-$) in the ^{20}Ne nucleus, confirming the results of Ref. 84. The calculated $W(\Omega_t,\Omega_\alpha)$ at ^{7}Li =45 MeV and θ_t=0° have a maximum at small angles θ_α, although the ratio and location of the ACF maxima corresponds to a squared Legendre polynomial only when the optical interaction in the exit channel is absent.

However, all these estimates of the effect of distortions in the reactions (^{6}Li,d) and (^{7}Li,t) were made by assuming that excited states of the final nuclei, the reaction products, can be described by wave functions of the discrete spectrum with minimum binding energy. This is permissible as a first approximation, especially since the sensitivity of the calculation to the choice of potential parameters of such a quasibound state was analyzed in Ref. 82 [the wave function of this state was found by a numerical procedure known as the well-depth prescription (WDP); Ref. 86]. Increase of the potential radius leads to a large spatial extent of the wave function of the $\alpha+^{12}$C bound state, which tends to increase the probability for particle separation, and therefore can effectively model a quasistationary state.

Nevertheless, the development of methods for describing the wave functions of high-lying quasistationary states more correctly remains one of the crucial problems in the theoretical analysis of angular correlations. Actually, in p- and sd-shell nuclei, most of the α-particle states lie above the α-particle separation threshold, i.e., these states are unbound or quasistationary. The wave functions describing such states must have an asymptote which includes the probability for α-particle emission, i.e., the finite width of the level to α decay.

Cluster wave functions for unbound states with divergent asymptote, the so-called Gamow wave functions, were used in Ref. 56 for calculating the cross sections of α-transfer reactions in the EFR DWBA. Gamow wave functions were used in Ref. 78 for analyzing the angular correlation functions in the (^{6}Li,d) reaction, and by us in Ref. 87 for the ^{12}C(^{7}Li,t)^{16}O*(α)^{12}C reaction. Next we shall briefly describe the main features of the method of calculating the wave functions of bound and quasistationary states.

5.2. Calculation of the wave functions of bound and quasistationary cluster states

The following factors must be taken into account when constructing the wave functions of the relative motion of the clusters at the decay vertices for bound and quasistationary nuclear states. First, the wave functions must be compatible with the spin selection rules and the conservation laws at the vertices, and also with the Pauli principle regarding permutations of nucleons among clusters. Second, the asymptote of the wave function must be chosen correctly, because the transfer reactions induced by semiheavy ions of relatively low energy mainly occur in the peripheral region of the nucleus. Third, the spectroscopic characteristics of the nucleus (the reduced widths of various cluster configurations) must be compatible with the wave functions obtained. In addition, the formation of highly excited states requires inclusion of phenomena related to their instability.

Beginning with the work of Gamow[88] on the theory of α decay, the study of the various aspects and properties of quasistationary states in nuclei has played an important role in nuclear spectroscopy and the theory of nuclear reactions. The analytic properties of the wave functions of quasistationary states and the production and decay of unstable particles have been studied intensively since the 1960s (Ref. 89).

Theoretical calculations of the cross sections for reactions induced by lithium ions with the formation of high-lying α-cluster states have been performed by the distorted-wave method with zero interaction range, using various methods of regularizing the radial overlap integrals of the "distorted" waves and the wave functions of resonance states. The procedure developed in Ref. 90 was used in Ref. 91 for narrow, low-lying resonances. For high-lying resonances an original method of calculation was developed by Vincent and Fortune.[92]

The cross sections for reactions associated with the formation of highly excited α-particle levels were calculated in Ref. 56 by introducing wave functions of the Gamow type which are numerical solutions of the stationary Schrödinger equation with complex energy eigenvalue.

For analyzing the angular correlations in reactions involving semiheavy ions in which high-lying states are excited, it is certainly interesting to be able to find a numerical solution of the Schrödinger equation with complex energy in

order to obtain Gamow-type wave functions, and to construct an algorithm for calculating the width of a narrow resonance corresponding to a given quasistationary energy level. A similar procedure used together with comparison of the calculated and experimental widths allows the spectroscopic factor to be obtained in a given decay channel of the quasistationary state.[93,94] Such a solution must describe quasidiscrete levels in the nuclear energy spectrum which satisfy the condition that the level width is smaller than the level spacing. Of course, the solution, a Gamow wave function, is weakly divergent, and so it cannot be normalized throughout space. However, as shown in Ref. 89, in a restricted region of space a nonrenormalizable function always approximates a normalized one. If it is assumed that the desired wave function preserves its normalization in the final, sufficiently large, volume, the upper limit on the normalization integral can be chosen.

The basic numerical method of solving the Schrödinger equation with complex energy is the method of the well-depth prescription (WDP) proposed in Ref. 86. It is used as the basis for numerically modeling the wave functions of bound states possessing definite symmetry, satisfying given selection rules, and having the correct asymptotic behavior. The WDP is widely used and incorporated in most of the contemporary computer programs for calculating the characteristics of direct nuclear reactions.

Let us consider the generalization of this method to the case of complex energy and wave functions.[41,87]

It is required to find the numerical solution of the Schrödinger equation with complex energy $E=E_0-i\Gamma/2$. The real part $E_0>0$ determines the energy of the excited nuclear level, and the imaginary part Γ is the width of this level. If the state in question has a pronounced cluster structure, i.e., if the wave function describes a quasistationary state of two nuclear clusters A and x in the nucleus B, then the energy E_0 is expressed in terms of the binding energy $\mathscr{E}_{Ax}$ of the clusters A and x in the nucleus B and the energy of the excited state E_B^* of the nucleus B:

$$E_0=\mathscr{E}_{Ax}+E_B^*=\mathscr{E}_B-\mathscr{E}_A-\mathscr{E}_x+E_B^*. \tag{42}$$

The equation for the radial wave function $u_l(\rho)$ with energy E and definite orbital angular momentum l has the form

$$\frac{d^2u_l(\rho)}{d\rho^2}-\left[\frac{V_N(\rho)}{E}-\frac{V_C(\rho)}{E}-\frac{l(l+1)}{\rho^2}-1\right]u_l=0. \tag{43}$$

Here we have used the notation $\rho=kr$ with $k=\sqrt{2mE}/\hbar$, m is the reduced mass of the particles, $V_C(\rho)$ is the Coulomb potential corresponding to the potential of a uniformly charged sphere of radius R_C (the Coulomb radius of the nucleus),

$$\frac{V_C(\rho)}{E}=\begin{cases}\dfrac{2\gamma}{\rho}, & \rho>\rho_C,\quad \rho_C=kR_C,\\ \dfrac{\gamma}{\rho}\left(3-\dfrac{\rho}{\rho_C}\right), & \rho<\rho_C,\end{cases}$$

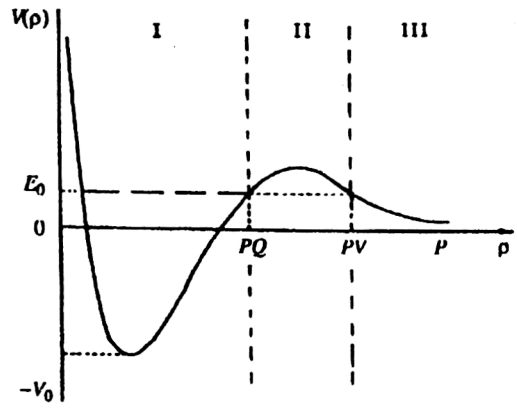

FIG. 1. Schematic depiction of the potential, including the nuclear, Coulomb, and centrifugal terms.

$\gamma=Z_1Z_2e^2/v$ is the Coulomb parameter, and $V_N(\rho)$ is the nuclear potential, which has the standard Woods–Saxon form.

The wave function $u_l(\rho)$ satisfies the normalization condition

$$\frac{1}{k^3}\int\rho^2u_l^2(\rho)d\rho=1. \tag{44}$$

The solution of Eq. (43) must describe quasidiscrete levels in the nuclear energy spectrum for which the following condition is satisfied: the level width must be smaller than the level spacing. Since the level width is related to the level lifetime, a quasistationary state is characterized by a finite (but large) lifetime, i.e., the nucleus decays with the emission of a particle.

The potential in which the particle of mass m moves can be depicted schematically as the nonmonotonic curve shown in Fig. 1. In view of the characteristic behavior of the potential $V(\rho)$, the entire interaction space can be divided into three regions. The wave functions in each region have a definite form and join smoothly at the boundaries.

In the first region the wave function describes the motion of the particle inside the potential well up to the point where the particle is reflected from the Coulomb barrier (point PQ), with the boundary condition $u_l(\rho)\to0$ for $\rho\to0$. For small ρ, $u_l^{\mathrm{I}}(\rho)$ is defined as an expansion, $u_l^{\mathrm{I}}(\rho)\simeq\rho^{l+1}$. Next, the method of iterations is used to select the width of the potential well for given geometrical parameters of the potential $V(\rho)$ such that the wave function $u_l^{\mathrm{I}}(r)$ in region I corresponds to a quantum state with given energy E, definite orbital angular momentum l, and a given number of nodes N [$N=\frac{1}{2}(n-l)+1$, where n is the principal quantum number]. Since ρ is complex, the function $u_l(\rho)$ is also complex.

In region II, which corresponds to the particle being below the Coulomb and centrifugal barrier, the solution of Eq. (43) takes the form

$$u_l^{\mathrm{II}}(\rho)=e^{-\rho}\rho^{-\gamma}\left(1+\sum_{i=1}^{\infty}\frac{a_{i+1}}{\rho^{i+1}}\right), \tag{45}$$

where

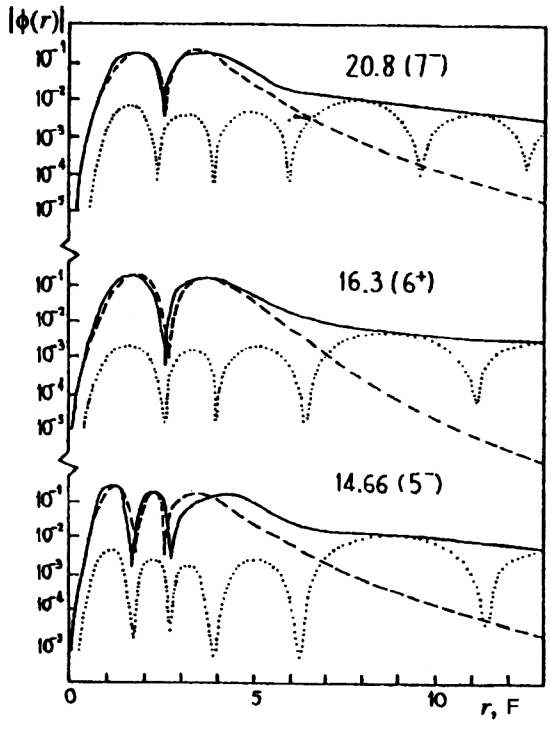

FIG. 2. Comparison of the Gamow and WDP wave functions $\phi_l(r) = u_l(r)/r$. The solid lines are the absolute values of the real parts of the Gamow wave functions. The dashed lines are the absolute values of the imaginary parts. The dot–dash lines are the WDP wave functions with fictitious binding energy $\varepsilon = -0.1$ MeV. The parameters of the calculation are given in Table I.

$$a_{i+1} = \frac{l(l+1)-(\gamma+i)(\gamma+i+1)}{2(\gamma+1)}\, a_i, \quad a_0 = 1.$$

The initial value at the outer boundary of region II, the point PV, is determined by Eq. (45). Equation (43) is then integrated in the reverse direction, from the point PV in the direction of decreasing ρ to the point PQ. The resulting function $u_l^{\mathrm{II}}(\rho)$ is matched to the solution $u_l^{\mathrm{I}}(\rho)$ at the point PQ.

In region III the particle emerges from under the potential barrier and is separated from the nucleus. Since the particle is created as a result of the decay of a quasistationary state, the solution in this region must be described by a wave function containing only an outgoing wave. We introduce the notation $\rho = \rho_{\mathrm{R}} - i\rho_{\mathrm{Im}}$, and then in region III we can write $u_l^{\mathrm{III}}(\rho)$ as

$$u_l^{\mathrm{III}}(\rho) = [F_l(\rho_{\mathrm{R}}) + iG_l(\rho_{\mathrm{R}})]e^{i\eta_l} e^{\rho_{\mathrm{Im}}}.$$

Here $F_l(\rho_{\mathrm{R}})$ and $G_l(\rho_{\mathrm{R}})$ are the regular and irregular Coulomb functions, respectively, and η_l is the Coulomb phase shift.

At the boundary of regions II and III the function $u_l^{\mathrm{III}}(\rho)$ is matched to the corresponding value of the function $u_l^{\mathrm{II}}(\rho)$.

The function $u_l(\rho)$ found in this manner is normalized by the condition (44). It diverges weakly at the asymptote, and so it cannot be normalized throughout space. However, it can be assumed that $u_l(\rho)$ retains its normalization in the final, sufficiently large volume, and the point PV can be chosen as the upper limit of the integral in (44).

In Fig. 2 we give the radial dependences of the probability density of unbound, high-lying α-cluster states: the terms of the rotational bands with $K^{\pi} = 0^+$ and 0^- in the ^{16}O nucleus for the Gamow wave functions and the wave functions of the relative motion of the clusters bound with a fictitious negative binding energy $\varepsilon_{\mathrm{b}} = -0.1$ MeV. We see from Fig. 2 that the considerable extent and magnitude of the Gamow wave functions in the asymptotic region owing to the inclusion of the imaginary part of the wave function, which models the α-particle tunneling through the potential barrier, gives a better representation of the cluster structure of excited levels of light nuclei.

According to R-matrix theory, the α width Γ_l^{α} of a resonance state is expressed in terms of the reduced width θ_l^2 and the penetration factor P_l: $\Gamma_l^{\alpha} = 2P_l\theta_l^2$.

The reduced width is related to the spectroscopic factor and the square of the radial part of the wave function of the relative motion at the point $r = a_{\mathrm{c}}$, where a_{c} is the channel radius, as[92]

$$\theta_l^2 = s_l \frac{2}{2\mu a_{\mathrm{c}}} |u_l(a_{\mathrm{c}})|^2.$$

Therefore, by calculating the so-called single-cluster α width[92]

$$\Gamma_l^{\alpha} = \frac{2}{2\mu a_{\mathrm{c}}} |u_l(a_{\mathrm{c}})|^2 2P_l \tag{46}$$

and comparing it to the experimental width Γ^{exp} of the resonance state, we find the spectroscopic factor S_l for the state in question:

$$S_l = \Gamma^{\mathrm{exp}}/\Gamma_l^{\alpha}. \tag{47}$$

After calculating the wave function in all space, the level width Γ_l is calculated using (46), in which the penetration factor P_l, equal to $ka_{\mathrm{c}}/(F_l^2(a_{\mathrm{c}}) + G_l(a_{\mathrm{c}}))$, and the wave function $u_l(\rho)$ are taken at $r = a_{\mathrm{c}}$, which corresponds to the conventional boundary of the nuclear interaction region.

In computer programs the level width is usually calculated as follows. Some reasonable value Γ_l^0 is specified, and the wave function $u_l^0(r)$ is found in all three regions. In the next approximation the width Γ_l^1 found from (45) is used, and the wave function $u_l^1(\rho)$ is determined again, and so on. The iteration process stops when two successive values of Γ_l^n differ by less than a specified small amount.

Some important features of this procedure for calculating the single-particle level width should be noted. First, the algorithm for calculating Γ_l is quite stable and rapidly convergent, and it uniquely determines the value of $\Gamma_l(a_{\mathrm{c}})$ for the given parameters of the problem. Second, the use of a numerical procedure for calculating the wave function in which the geometrical parameters of the nuclear potential are fitted quantities leads to a significant uncertainty in the calculated Γ_l. A change of the geometry of the potential well for a given level location leads to a significant change of the well depth and the height of the potential barrier. This undoubtedly also affects Γ_l. In Fig. 3 we show the dependence of the width Γ_l on the radius r_0 and the diffuseness a of the nuclear potential $V_{\mathrm{N}}(r)$. We see from this figure that as r_0 and a increase, i.e., as V_0 decreases, the value of Γ_l in-

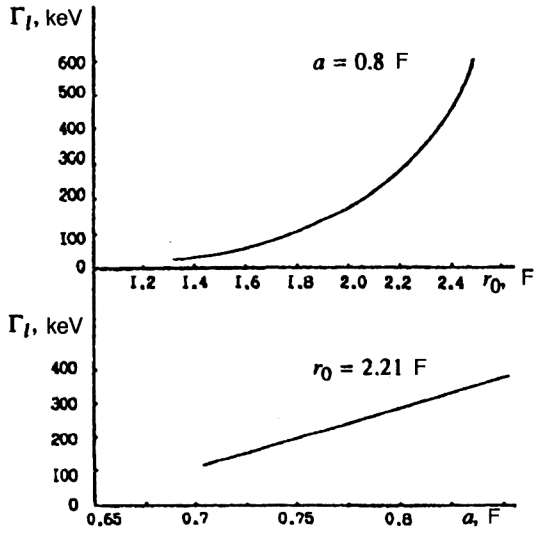

FIG. 3. Dependence of the width Γ_l of the 7^-, $E^*=13.69$ MeV level, $r=r_0A^{1/3}$, on the geometrical parameters of the nuclear potential.

creases. However, for given potential parameters the width Γ_l can be determined fairly accurately, i.e., the uncertainty in the calculated Γ_l associated with the choice of channel radius a_c characterizing the nuclear boundary or the boundary of the region where the nuclear potential acts is eliminated. In Fig. 4 we show the dependence of the width $\Gamma_l(r)$ calculated using (46) on the choice of the point a_c. We also show the behavior of the nuclear potential $V_N(r)$ (as the ratio to V_0 in percent) in this region. The nonmonotonic curve describing the dependence $\Gamma_l(r)$ has a maximum in the region of exponential (by roughly a factor of ten) falloff of the nuclear potential. The location of this maximum determines the point a_c at which the width $\Gamma_l(a_c)$ is calculated.

In spite of the dependence of the calculated Γ_l on the parameters of the calculation, there are various methods of making the given parameters consistent with the physical ideas about the wave functions of quasistationary states. One of these is the relation between the decay width of the α-particle quasistationary state calculated by the method described above, the experimental width $\Gamma_\alpha^{\exp}$ of this level due to α-particle emission, and the spectroscopic factor S_l given by (47).

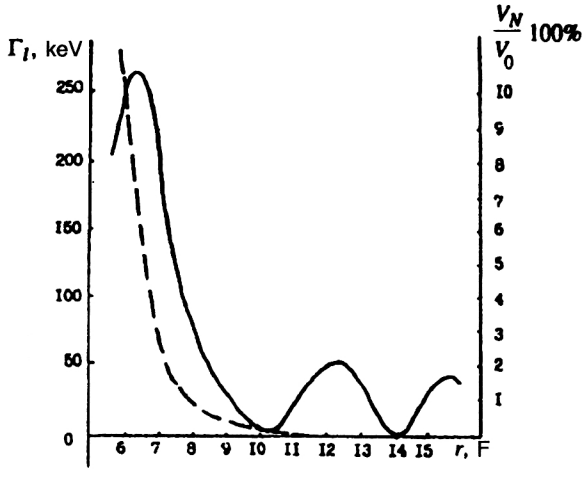

FIG. 4. Dependence of the calculated width Γ_l on the radius r of the nuclear interaction region (solid line). The dashed line is the dependence of the nuclear interaction potential on r (as the ratio to the depth V_0 in percent).

In Tables I and II we give the values of the calculated α widths Γ_l^α, the spectroscopic factors S_l, the channel radii a_c at which the Γ_l^α were calculated, and also the geometrical parameters and depths V_0 of the Woods–Saxon nuclear potential for unbound α-cluster states—the terms of the bands with $K^\pi=0^+$ and 0^- in ^{16}O and the three bands with $K^\pi=0^-$, 0_1^+, and 0_2^+ in ^{20}Ne. The values of $\Gamma^{\exp}$ and S^{DWBA} are taken from Ref. 44.

We see from Table I that, in spite of the considerable spread of the experimental widths for different levels with $K^\pi=0^+$ and 0^-, the calculated values of the spectroscopic factors turn out to be very stable and characterize the levels of a given band.

From Table II we see that for a fairly wide range of ^{20}Ne excitation energies it is possible to obtain good agreement between the calculated S_l and the experimental values, while allowing variation of the nuclear potential parameters within a reasonable range.

In our subsequent calculations of the reaction cross sections we shall focus on these values of S_l and compare them with the values of the spectroscopic factors obtained by normalization of the experimental and calculated cross sections.

5.3. Theoretical analysis of the differential cross sections and angular correlation functions in the (^{6}Li,d) and (^{7}Li,t) reactions with the formation of quasistationary α-cluster states

The theoretical analysis of $d-\alpha$ and $t-\alpha$ angular correlations in the (^{6}Li,d) and (^{7}Li,t) reactions with the formation of high-lying α-cluster states in $p-sd$-shell nuclei is based on current models of nuclear reactions and computer programs and allows the analysis of problems arising in experimental studies. The most important of these is the problem of the consistency of the experimental angular correlation functions and the available data on the differential cross sections of the (^{6}Li,d) and (^{7}Li,t) reactions. Here it is necessary to explain the nature of the simple angular dependence of the ACFs observed in most experiments, to study the role of plane-wave distortions as a function of the incident ion energy and the excitation energy of the final nucleus, and to understand the features of the interaction of semiheavy ions leading to the formation of high-lying cluster states.

As noted earlier in this review, the most suitable and, at present, widely used models for describing nuclear reactions of this type are the model of direct transfer of an α-particle cluster and the statistical model of compound-nucleus formation.

We have performed such an analysis in Ref. 87, including a complex study of the differential and doubly differential cross sections ($t-\alpha$ angular correlation functions) in the reaction ^{12}C(^{7}Li,t)^{16}O*(α)^{12}C for the purpose of answering the questions posed above, and also for studying the spectroscopic characteristics of quasistationary states—the terms in the $K=0^+$ and 0^- rotational bands in ^{16}O—and the interac-

TABLE I. Parameters of α-cluster states in ^{16}O, potentials, and wave functions of the relative motion. $V(\mathbf{r})=V_0 f(\mathbf{r})$, where $f(\mathbf{r})=(1+\exp(\mathbf{r}))^{-1}$, $\mathbf{r}=(r-R_0)/a$, $R_0=2.52$ F.

K^π	I^π	N[1]	E^*, MeV	ε, MeV	V_0, MeV	a, F	a_c, F	Γ,[2] keV	Γ^α, keV	$S=\Gamma/\Gamma_\alpha$
0^+	4^+	2	10.35	3.19	169.5	0.65	6.2	30	18.5	1.60
	6^+	1	16.30	9.14	163.0	0.65	5.2	300	246.5	1.22
0^-	3^-	3	11.59	4.43	188.0	0.60	5.6	700	716.0	0.98
	5^-	2	14.66	7.50	195.4	0.60	5.0	500	457.0	1.09
	7^-	1	20.80	3.64	196.0	0.60	5.0	500	519.0	0.96

[1] N is the number of nodes of the radial wave function.
[2] Data from Ref. 44.

tion mechanism of semiheavy ions leading to the formation of high-lying α-cluster states.

The following experimental data were fundamental for our analysis: the differential cross sections of the reaction ^{12}C(^{7}Li,t)^{16}O measured in Ref. 71 at $E_{\text{Li}}=38$ MeV for various excited states in ^{16}O up to $E^*=(7^-)$ 20.7 MeV and the $t-\alpha$ angular correlation functions from the reaction ^{12}C(^{7}Li,t)^{16}O*(α)^{12}C at $E_{\text{Li}}=45$ MeV measured in Ref. 83. A feature of the experimental ACFs for levels with I_f equal to 5^- (14.66 MeV), 6^+ (16.3 MeV), and 7^- (20.7 MeV) is the fact that at triton emission angles θ_t close to 0° (in the experiment, $\theta_t^{\text{lab}}=10°$), the form of the ACFs is reproduced well by the square of the Legendre polynomial of order I_f, which corresponds to the plane-wave approximation. As shown in Ref. 14, the DWBA calculations including distorting optical potentials in the entrance and exit channels cannot reproduce this experimental fact.

Therefore, the simultaneous analysis of all the experimental data is needed in order to understand whether or not it is possible to obtain an adequate description of the differential cross sections and experimental ACFs for a single set of optical potential parameters and functions describing the relative motion of the clusters.

Studies of the differential cross section for the reaction ^{12}C(^{7}Li,t)^{16}O* with the formation of low-lying levels in ^{16}O which are coupled with respect to α-particle emission[71,72] have shown that in this case the main reaction mechanism is direct transfer of an α-particle cluster. Meanwhile, it is necessary to adequately take into account the contribution of the statistical mechanism to the cross section for this reaction, because at triton emission angles $\theta_t>90°$ it dominates and determines the behavior of the differential cross section.

Let us begin by defining the parameters used in the calculations. The optical potential for the interaction of ^{7}Li and ^{12}C at $E_{\text{Li}}=36$ MeV selected in Ref. 95 was also used in Refs. 72 and 96 to calculate the cross sections for this reaction, and we took it as the starting point. The optical potential in the exit channel of the reaction is less well defined, because, in general, it must vary, depending on the degree of excitation of the final nucleus. In these calculations we shall start from the most general recommendations of Ref. 97. The optical-potential parameters are given in Table III.

In order to reliably estimate the $\alpha+^{12}$C spectroscopic factors in various states of ^{16}O and also to describe the reaction cross section at angles $\theta_t>90°$, as a first step it is necessary to calculate the contribution to the cross section from the statistical mechanism of compound-nucleus formation. Detailed calculations for the reaction ^{12}C(^{7}Li,t)^{16}O were performed in Ref. 71 for ^{16}O states up to $E^*=20.7$ MeV (7^-) and in Ref. 96 up to $E^*=11.10$ MeV. In Ref. 71 the calculated cross section was normalized to the 2^- (8.87 MeV) level, and in Ref. 96 an effective normalization was used, i.e., the cross section was decreased by cutting off the sum of partial cross sections at the critical angular momentum l_c. As shown in Ref. 98, the critical angular momentum l_c, and also the critical total angular momentum $\mathbf{I}_c=\mathbf{l}_c+\mathbf{I}_a+\mathbf{I}_A$, in the semiclassical approximation characterize the maximum angular momentum in the entrance channel at which complete fusion of the initial nuclei, i.e., compound-nucleus formation, can still occur.

TABLE II. Parameters of α-cluster states in ^{20}Ne, potentials, and wave functions of the relative motion. $V(\mathbf{r})=V_0 f(\mathbf{r})$, where $f(\mathbf{r})=(1+\exp((r-r_0)/a))^{-1}$, $r=r_0(A^{1/3}+x^{1/3})/a$.

K^π	I^π	E^*, MeV	ε, MeV	V_0, MeV	r_0, F	R, F	a, F	Γ,[1] keV	Γ^α, keV	S	S^{DWBA1}
0^-	1^-	5.78	1.05	90.13	0.95	9.30	0.80	0.028	0.061	0.46	0.54
	3^-	7.16	2.43	86.27	0.95	6.80	0.80	8.20	33.7	0.24	0.26
	5^-	10.26	5.53	78.23	0.95	7.20	0.80	145.0	604.0	0.24	0.15
	7^-	13.36	8.96	74.81	0.95	6.40	0.80	310.0	590.0	0.53	
0_1^+	6^+	8.78	4.05	130.68	0.70	7.50	0.75	0.11	0.46	0.24	0.20
	8^+	11.95	7.22	154.74	0.65	7.10	0.70	0.035	0.077	0.45	0.51
0_2^+	2^+	7.42	2.68	50.21	0.85	6.80	0.80	15.0	113.0	0.13	0.13
	4^+	9.99	5.26	50.23	0.85	6.40	0.80	155.0	584.0	0.27	
	6^+	12.59	7.86	50.49	0.85	5.80	0.80	72.0	145.0	0.49	
	6^+	13.11	8.38	48.87	0.85	5.60	0.80	102.0	256.0	0.40	

[1] Data from Ref. 44.

TABLE III. Optical-potential parameters and parameters for calculations in the Hauser–Feshbach formalism.

Channel	V, MeV	R_V, F	a_V, F	W_I, MeV	R_I, F	a_I, F	Type	R_{Coul}, F	a, MeV^{-1}	Δ, MeV	Y	E_c, MeV
$n+^{18}F$	38.62	3.380	0.660	7.93	3.284	0.480	sur	0.00	2.818	0.00	0.27	5.86
$p+^{18}O$	35.43	3.280	0.650	13.50	3.284	0.470	sur	3.28	3.167	6.73	0.27	8.38
$d+^{17}O$	89.27	2.707	0.752	6.52	3.500	0.812	sur	3.34	2.630	2.30	0.30	6.02
$t+^{16}O$	170.00	2.870	0.723	20.00	4.030	0.800	vol	3.125	1.890	4.37	0.33	10.4
$\alpha+^{15}N$	130.00	3.380	0.625	44.92	3.377	0.350	vol	3.45	2.558	0.28	0.37	11.5
$^{5}He+^{15}N$	17.36	5.560	0.450	3.48	5.560	0.450	vol	3.13	2.030	0.00	0.41	8.63
$^{5}Li+^{14}C$	17.18	5.560	0.450	3.43	5.560	0.450	vol	3.05	2.177	3.23	0.41	8.87
$^{6}Li+^{13}C$	234.00	2.770	0.760	10.30	4.580	0.640	sur	5.87	2.372	3.44	0.47	8.21
$^{7}Li+^{12}C$	245.00	2.770	0.759	14.70	4.580	0.909	vol	2.98	1.050	10.33	0.53	11.2
$^{8}Be+^{11}B$	26.20	5.280	0.950	25.00	5.280	0.950	vol	5.55	1.674	3.02	0.62	10.1

We used the CNCOR code,[41] described in Sec. 4.2 above, to calculate the contribution of the compound-nucleus formation mechanism to the reaction cross section. In the calculation of the total width $g(I_f)$ of decay of the compound nucleus via all open channels [Eq. (31)] we summed the contribution of the individual known discrete levels, while the continuum contribution was calculated by integrating over energy, taking into account the level density beginning at energy E_c, the edge of the continuum. The actual value of E_c corresponds to the nuclear excitation energy at which separation of one of the particles of the nucleus becomes possible. The yrast-line cutoff was made by taking into account the relation $E_I = YI(I+1)$, where $Y = 2\hbar/F_s$; $F_s = \frac{2}{5} r_0^2 A^{5/3}$ is the moment of inertia of a solid sphere.

The Fermi-gas model with parameters proposed in Ref. 47 was used to describe the nuclear level density. All the parameters used in the calculation of the total decay width, the level densities, and the optical potentials are given in Table III.

The starting point was the calculation of the reaction cross section for the 2^- (8.87 MeV) excited state in ^{16}O, the population of which via direct single-stage mechanisms is forbidden by selection rules. Having defined the model parameters in this manner, we calculated the cross sections for several states in ^{16}O, assuming that for the given incident particle energy the critical angular momentum I_c is less than $12\hbar$ (Ref. 96).

In Fig. 5 we compare the differential cross sections (dotted lines) for the $^{12}C(^{7}Li,t)^{16}O$ reaction, calculated using the statistical model, with the experimental data from Ref. 71. Both the shape and the absolute value of the characteristic statistical angular distribution of tritons with excitation of the 2^- (8.87 MeV) level are reproduced well. In addition, our calculations can explain the differential cross sections at

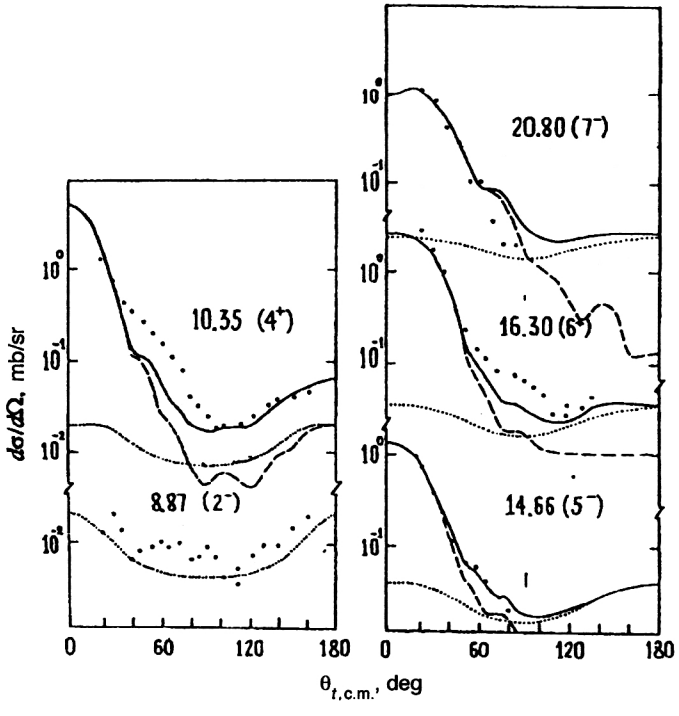

FIG. 5. Differential cross sections of the reaction $^{12}C(^{7}Li,t)^{16}O^*$ for $E_{Li} = 38$ MeV. The solid lines are the total theoretical cross section, the dashed lines are the contribution of the direct α-transfer mechanism, and the dotted lines are the contribution of the compound-nucleus formation mechanism. The experimental points are from Ref. 71.

large angles θ_t for states which are strongly populated at forward angles. However, the cross sections at small angles θ_t cannot be explained within the statistical theory; their explanation requires the theory of direct reactions.

Calculations of the characteristics of the $^{12}C(^7Li,t)^{16}O$ reaction for the direct α-transfer mechanism were performed in the EFR DWBA using the OLYMP-5 code.[41] Special attention was paid to the study of the high-lying quasistationary α-cluster states in ^{16}O belonging to the $K^\pi=0^+$ and 0^- rotational bands.

Our earlier analysis[99] of this reaction with incident ^7Li ion energy equal to 21 MeV for the ground state and the 4^+ (10.35 MeV) state showed that of the two single-stage direct mechanisms associated with the breakup of ^7Li, the most important is cluster stripping. Heavy substitution is suppressed by several orders of magnitude. This conclusion remains unchanged for the higher ^7Li energies studied, and so the rest of the calculations will be performed only for the mechanism of cluster stripping of the α particle.

Let us see how the choice of wave functions of the cluster relative motion affects the differential cross section and the angular correlation function, and also compare the values of the spectroscopic factors S_l^α obtained in Sec. 5.2 and in the calculation of the reaction cross sections.

The ^7Li cluster wave function and its overlap with the $\alpha+t$ interaction potential have been studied in detail by many authors. In addition, in Ref. 100 a comparison was made of the overlap functions $W(\mathbf{r}_{bx})=\langle\Phi_b\Phi_x|V_{bx}|\Phi_a\rangle_{\mathbf{r}_{bx}}$ of the interaction potential V_{bx} of the nuclei b and x with the nuclear internal wave functions Φ calculated in the microscopic model of generator coordinates with various nucleon–nucleon forces and in the DWBA using local phenomenological potentials and bound-state functions. In addition, the cross sections for the $^{12}C(^7Li,t)^{16}O$ reaction calculated in the DWBA with phenomenological and microscopic potentials were compared. The calculations showed that, in spite of significant differences in the behavior of $W(\mathbf{r}_{bx})$, the cross sections calculated using various potentials are in surprisingly good agreement with each other, particularly in the forward hemisphere of triton emission. It is only at large angles θ_t that discrepancies in both the magnitude and the form of the cross sections are observed. Comparison of the results of our calculations with the results given in Ref. 100 confirmed the conclusion that the cross section for the $^{12}C(^7Li,t)^{16}O$ reaction in the forward hemisphere is weakly sensitive to the choice of the $\alpha-t$ interaction parameters, and justified the use of the parameters selected earlier in our analysis of reactions involving α particles on lithium nuclei:[101] $V_0=46$ MeV, $R_0=3.18$ F, and $a=0.9$ F. The corresponding $\alpha-t$ spectroscopic factor was taken, as in Ref. 71, to be 0.95 for the rest of the calculations. The parameters of the potential and the wave function of the $\alpha+^{12}C$ bound state in ^{16}O are given in Table I.

In Fig. 5 we compare the theoretical differential cross sections (solid lines) with the experimental data from Ref. 71 (circles). As seen from this figure, the triton angular distributions for states in ^{16}O belonging to the $K^\pi=0^+$ and 0^- bands are determined by the α-cluster stripping mechanism

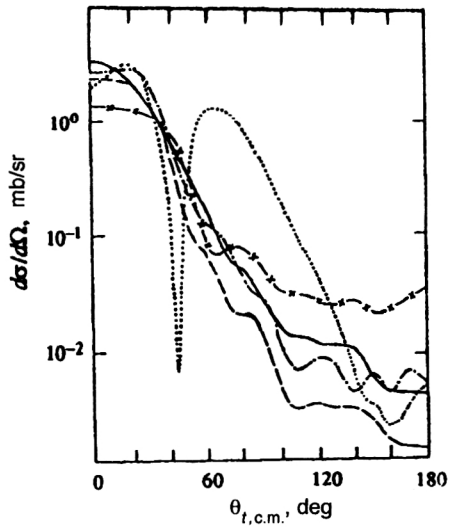

FIG. 6. Differential cross section of the reaction $^{12}C(^7Li,t)^{16}O^*$, $I_f=6^+$, for $E_{Li}=38$ MeV. The calculations were performed in the EFR DWBA for the direct α-transfer mechanism with various bound-state wave functions and with optical potentials with various parameters (see Table IV). The solid line is version 1 with Gamow wave function; the dotted line is version 1 with weakly coupled wave function; the dot–dash line is version 2 with Gamow wave function; the curve with the crosses is version 2 with weakly coupled wave function. The dotted line is the calculation in the plane-wave approximation.

in the forward hemisphere of the angles θ_t. At angles $\theta_t>90°$ the main contribution comes from the statistical mechanism of compound-nucleus formation. The poorest agreement with experiment is obtained at intermediate triton emission angles, which might be related to the neglected contribution of processes intermediate between direct and statistical ones.

Our study of the role of optical potentials which distort the incoming and outgoing plane waves in the formation of a strongly excited final nuclear state has shown that the differential cross sections calculated for this reaction with the direct α-cluster transfer mechanism are weakly sensitive to a significant change of the model parameters.

This can be illustrated for the example of calculating the differential cross section of the reaction for the 6^+ (16.30 MeV) level (Fig. 6). The differential cross sections shown in this figure were calculated in the EFR DWBA for the α-particle stripping mechanism and normalized to the experimental values. We see that the shape of the triton angular distribution at angles $\theta_t<90°$ is weakly sensitive to great weakening and even total shutoff of the interaction in the exit channel, and also to decrease of the depth V_0 of the real part of the optical potential in the entrance channel. The cross section at angles $\theta_t>90°$ is more sensitive to the choice of parameters; in particular, a decrease of the depth W_0 of the imaginary part, i.e., weakening of the absorption in the entrance channel, leads to a significant increase of the cross section in the backward hemisphere of triton emission. However, at angles $\theta_t>90°$ a significant or even dominant role is played by other, nondirect, reaction mechanisms. The cross section calculated in the plane-wave approximation and also with only a Coulomb interaction in the entrance and exit channels fundamentally differs from the experimental one.

TABLE IV. Dependence of the spectroscopic factor S_l and population of the zero projection $P_0(\theta_t=0°)$ on the depth of the real part V_0 and the imaginary part W_0 of the optical potential in the entrance and exit channels of the reaction $^{12}C(^7Li,t)^{16}O^*$ for $E_{Li}=38$ and 45 MeV.

No. of OP	I_f^*	E^*, MeV	Type of $\Psi(^{16}O)$	38 MeV		45 MeV
				S_l	P_0,%	P_0,%
1	4^+	10.35	Gamow	3.00	52.6	56.7
1			weakly coupled	2.50	37.3	49.5
2			Gamow	1.80	76.5	85.0
2			weakly coupled	1.00	63.9	70.9
3			Gamow	1.30	86.5	91.2
1	5^-	14.66	Gamow	0.46	18.5	39.6
1			weakly coupled	1.00	18.7	30.0
2			Gamow	0.26	44.0	76.9
2			weakly coupled	0.36	32.3	49.1
3			Gamow	0.21	61.0	82.0
1	6^+	16.30	Gamow	1.23	27.1	35.6
1			weakly coupled	1.60	11.7	22.4
2			Gamow	0.59	30.2	54.3
2			weakly coupled	0.80	18.5	32.6
3			Gamow	0.56	47.9	66.3
4			Gamow	0.53	35.7	66.9
5			Gamow	0.50	59.5	76.3
5			weakly coupled	0.75	42.0	71.0
1	7^-	20.80	Gamow	0.80	7.3	12.8
3			Gamow	0.19	12.6	41.3
5			Gamow	0.10	23.8	57.3
6			Gamow			69.6

The cross sections given in Fig. 5 have different absolute values, as is clear from the spectroscopic factors given in Table IV and obtained by normalization of the total (the direct plus the statistical mechanism) cross section to the experimental one. The values of S_l systematically decrease as the nuclear interaction is weakened.

We also note that the calculated differential cross sections are weakly sensitive to replacement of the Gamow wave functions of the relative motion by weakly coupled wave functions with fictitious binding energy $\varepsilon_b=-0.1$ MeV.

Therefore, on the basis of only analysis of the angular distributions it is impossible to state a clearcut criterion for choosing the parameters of the optical potentials, the wave functions of the relative motion, and, in the end, the spectroscopic factor S_l.

Turning now to analysis of the $t-\alpha$ angular correlation functions, we observe a qualitative change in the situation.

In Fig. 7 we give the ACFs for the 6^+ (16.30 MeV) level calculated at $E_{Li}=45$ MeV using the same approximations as for the differential cross sections shown in Fig. 6. We see from Fig. 7 that it is possible to obtain satisfactory agreement with experiment when not only the nuclear but also the Coulomb interaction is absent in the exit channel, i.e., for the plane-wave approximation in the exit channel, and also for weaker nuclear interaction in the entrance channel.

Our calculations have shown that the $t-\alpha$ angular correlation functions are considerably more sensitive to distortions of the plane waves in the formation of high-lying states than are the differential cross sections. At the same time, the population of the magnetic sublevels of a state with angular momentum I_f, which in our case is given, on the basis of (24), by

$$P^{I_f}_{M_f}=\frac{\Sigma_{M_2}|M_{I_fM_2M_f}|^2}{\Sigma_{M_2M_f}|M_{I_fM_2M_f}|^2}, \tag{48}$$

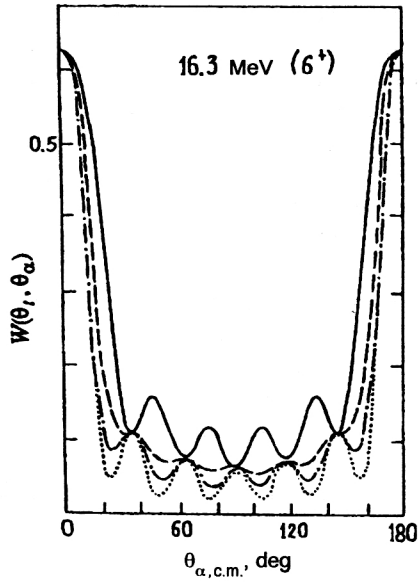

FIG. 7. The $t-\alpha$ angular correlation function in the reaction $^{12}C(^7Li,t)^{16}O(\alpha)^{12}C$ for $E_{Li}=45$ MeV. The calculations were performed in the EFR DWBA for the direct α-transfer mechanism with optical potentials with various parameters (see Table IV). The solid line is for version 1, the dashed line is for version 2, and the dot–dash line is for version 3.

is directly related to the behavior of the ACFs and is also sensitive to the choice of interaction in the entrance and exit channels.

As shown above in Sec. 5.1, in the plane-wave approximation for reactions with direct α transfer on nuclei with zero spin at $\theta=0°$, Eq. (40) for $M_{I_f M_2 M_f}$ contains only the term with $M_2=M_f=0$. Here $P^{I_f}_{M_f}=P^{I_f}_0=1$, i.e., only the zero spin projection of the emitted particle is populated, and the ACF is proportional to the square of the Legendre polynomial of order I_f. The degree of population of the zero projection of the angular momentum I_f therefore characterizes the polynomial behavior of the ACF at $\theta=0°$.

In Table IV we give the calculated populations $P^{I_f}_M$ for $M_f=0$ (P_0) for various optical-potential parameters and using Gamow or weakly coupled wave functions for the high-lying states in ^{16}O for E_{Li} equal to 38 and 45 MeV, respectively. In those cases where $P_0(\theta_t=0)$ is larger than 50%, $W(0,\theta_\alpha)$ approaches a form proportional to $[P_{I_f}(\cos\theta_\alpha)]^2$. The following versions of the calculations were performed: (1) using the optical potential of Table III in the entrance and exit channels of the reaction; (2) using the optical potential in the entrance channel but not in the exit channel; (3) using the optical potential in the entrance channel and plane waves in the exit channel, and also using the optical potential in the entrance channel weakened by a factor of two (versions 4 and 5) or four (version 6), and without the optical potential (version 4) or plane waves (versions 5 and 6) in the exit channel.

The ACFs for the 4^+ (10.35 MeV) state at $E_{\mathrm{Li}}=38$ and 45 MeV when the optical potential is present has a smooth, nearly nonoscillatory behavior. If there is no optical potential in the exit channel, the ACF for $I_f=4^+$ acquires a polynomial form, and the differential cross section gives a fairly good description of the experimental points (see Fig. 5). The spectroscopic factor obtained from normalization of the theoretical cross section to the experimental one (Table IV, version 2), equal to 1.8 for the Gamow wave functions, is in good agreement with the S factor of Table I, equal to 1.6.

For the higher-lying 5^- (14.66 MeV) state, a polynomial form of the ACFs at $E_{\mathrm{Li}}=45$ MeV is obtained when there is no nuclear interaction in the exit channel (the calculated curve in Fig. 8a corresponds to version 2 from Table IV), while at $E_{\mathrm{Li}}=38$ MeV it is obtained only with the plane-wave approximation in the exit channel. The behavior and magnitude of the differential cross section are hardly changed. The theoretical angular distribution for the 5^- state, shown in Fig. 5, corresponds to version 3 of Table IV and $S_l=0.21$.

The ACFs for the 6^+ (16.30 MeV) state at $E_{\mathrm{Li}}=45$ MeV, shown in Fig. 8b, correspond to versions 3 and 4 of Table IV. We see that satisfactory agreement with experiment can be obtained only if the nuclear interaction is absent in the exit channel and is weakened in the entrance channel. For $E_{\mathrm{Li}}=38$ MeV the polynomial form of the ACFs is obtained only when the plane-wave approximation is used in the exit chanel and the nuclear interaction in the entrance channel is weakened by more than a factor of two (version 5 of Table IV). The differential cross section for the 6^+ state in Fig. 5 corresponding to this variant has the spectroscopic factor $S_l=0.50$.

For the highest-lying α-cluster state, 7^- (20.8 MeV), a polynomial form of the ACF and population $P^7_0\approx 70\%$ at $E_{\mathrm{Li}}=45$ MeV can be obtained when the depth V_0 of the real part of the optical potential in the entrance channel is decreased significantly and the nuclear and Coulomb interactions in the exit channel are absent. For these parameters the differential cross section for $E_{\mathrm{Li}}=38$ MeV differs significantly from the experimental value. The theoretical differential cross section for the 7^- level (Fig. 5) can be obtained when the optical potential is included in the entrance channel but not in the exit channel (this corresponds to version 3 from Table IV and $S_l=0.19$). For $E_{\mathrm{Li}}=38$ MeV the zero spin projection is only 12% populated, and the ACF does not have a maximum at $\theta_t=0$, i.e., it is not described by the square of a Legendre polynomial.

On the basis of this analysis we arrive at the following conclusions.

1. The description of the observed polynomial form of the ACFs at $E_{\mathrm{Li}}=45$ MeV for high-lying states in ^{16}O requires weakening of the nuclear interaction in the entrance and exit channels. The degree of weakening depends on the excitation level of the final nucleus: as the excitation energy increases, the nuclear interaction is weakened and then becomes absent in the exit channel, while for the highest-lying states in ^{16}O ($I_f>5$) greater and greater weakening of the optical potential is observed also in the entrance channel.

2. At lower incident ion energy $E_{\mathrm{Li}}=38$ MeV, a polynomial form of the ACFs can be obtained for the same high-lying states in ^{16}O only when the nuclear interaction is weakened more than at $E_{\mathrm{Li}}=45$ MeV. A fairly good description of the differential cross sections can also be obtained in this case. However, for the α-cluster 7^- (20.8 MeV) state in ^{16}O it is impossible to obtain an adequate description of the differential cross section and a polynomial form of the ACF for $\theta_t=0$ at $E_{\mathrm{Li}}=38$ MeV. We therefore suggest that for this state [in view of the absence of data at this energy for the (^{7}Li,t) reaction] there is a suppression of the intensity of the first maximum in the $\alpha-t$ correlation function analogous to that observed in the (^{6}Li,d) reaction.[81]

3. The use of Gamow wave functions instead of weakly coupled ones noticeably improves the agreement between the calculated and experimental ACFs. Weakly coupled wave functions can be used for $E_{\mathrm{Li}}=38$ MeV only for the 4^+ (10.35 MeV) state. They cannot be used for the higher-lying states with $I_f=5^-$, 6^+, and 7^- because they require the introduction of the plane-wave approximation in both the exit and entrance channels.

Therefore, this analysis suggests that, first, the population P_0 and the form of the ACFs in (^{7}Li,t) reactions depend on the energy of the incident nucleus (this can be checked experimentally, although so far there are no data on the ACFs at various lithium energies). Second, for the α-transfer reaction with the formation of high-lying cluster states the interaction strength in the entrance channel depends on the degree of excitation of the nucleus, while for a given excited state it depends on the incident ion energy.

Comparing the spectroscopic factors S_l for α-particle

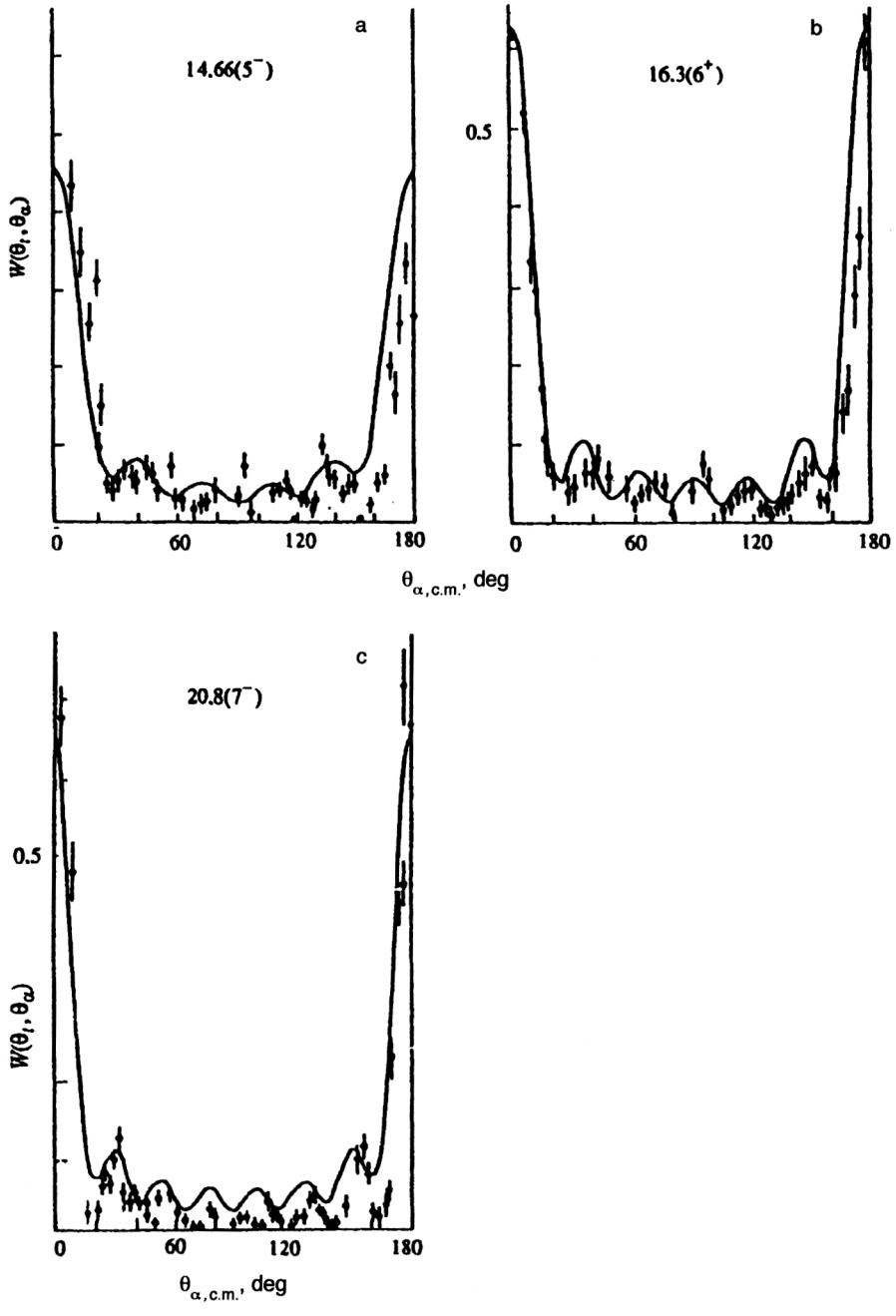

FIG. 8. The $t-\alpha$ angular correlation function in the reaction $^{12}C(^7Li,t)^{16}O(\alpha)^{12}C$ for $E_{Li}=45$ MeV. The solid lines are the EFR DWBA calculations for the direct α-transfer mechanism at $\theta_t=0°$. The experimental points are from Ref. 83.

separation from the ^{16}O nucleus in high-lying states, obtained from the model using Gamow wave functions (Table I) and from comparison of the theoretical and experimental cross sections (Table IV), we see that the spread of the values for the two cases is small, although the values of S_l obtained from comparison with experiment are several times smaller than the model ones. The two values obtained for S_l are closest for the lowest-lying state, the 4^+ (10.35 MeV) level, where a successful description of the reaction characteristics can be obtained also when the ordinary weakly coupled wave function is used.

This complicated analysis of the differential cross sections and $t-\alpha$ angular correlation functions from the reaction $^{12}C(^7Li,t)^{16}O^*(\alpha)^{12}C$ with the formation of high-lying α-cluster states in ^{16}O has shown that the features of the quasielastic mechanism responsible for fast-fragment formation in the α-transfer reaction are clearly manifested in this reaction. It can be interpreted within the spectator model,[102,103] in which the interaction of the emitted fragment (in our case, a triton) with the system $(x+A)$ formed in the final state, i.e., with the ^{16}O nucleus, is neglected. This feature of the $(^7Li,t)$ reaction, associated with the clearly expressed cluster structure of the ^7Li nucleus, has been noticed earlier in studying the angular correlations in the reaction $^{16}O(^7Li,t)^{20}Ne(\alpha)^{16}O$ (Ref. 13), and also in Ref. 74. Naturally, as the excitation of the final nucleus increases, the spectator properties of the emitted fragment are manifested more clearly, until the wave function becomes a plane wave.

Another feature of this process should be mentioned. As the excitation energy of the final nucleus increases, not only

the interaction between the nucleus and the emitted particle but also the interaction in the entrance channel becomes weaker. This is shown by the behavior of the $t-\alpha$ angular correlation function at small triton emission angles. The reaction differential cross sections calculated by taking into account this decrease of the depth of the optical potential in the entrance channel also agree satisfactorily with the experimental data.

This result appears paradoxical for the DWBA, a stationary model of the nuclear reaction in which the reaction is divided into three distinct, independent stages: entrance channel, instantaneous effect, and exit channel. We are seeing that the second reaction stage, the formation of the excited system $(x+A)$, affects the interaction in the first stage $a+A$, in the entrance channel. Apparently, here we are seeing the transition from a stationary description of the reaction to a dynamical one which explicitly takes into account the time dependence of the interaction. The following self-interaction mechanism arises in the strong excitation of the nucleus. The incident ion located in the field of the nucleus changes its self-consistent potential, which again acts on the incident ion. In the stationary picture we model this mechanism by decreasing the depth of the optical potential in the entrance channel relative to the optical-potential parameters obtained for ion elastic scattering and suitable for describing the interaction in weakly excited systems.

This self-interaction mechanism clearly depends on the incident ion energy, and it is associated with the significant energy dependence of the calculated angular correlation functions.

6. STUDY OF THE STATISTICAL AND DIRECT MECHANISMS IN THE $^{12}C(^{14}N,d)^{24}Mg$ REACTION BY THE METHOD OF $d-\alpha$ ANGULAR CORRELATIONS

The first results of studies of nuclear reactions induced by accelerated nitrogen ions at incident energies of up to 100 MeV on $1p$-, $2s-1d$-shell nuclei performed in the early 1970s (Refs. 104 and 105) suggested that these reactions could be treated as ones involving the transfer of large groups of nucleons. Nevertheless, after further analysis of the spectra, the excitation functions, and the angular distributions and, in particular, the observation of correlations of resonance-like structure in the excitation functions from elastic scattering and from reactions, it was concluded that the mechanism of compound-nucleus formation plays the dominant role in these reactions.[38,106,107]

In the statistical model of compound-nucleus formation in the Hauser–Feshbach formalism, special attention has been given to the concept of a critical angular momentum in the entrance channel I_{cr}. This is the maximum angular momentum possible in the fusion of two nuclei.[98,108] The introduction of I_{cr} into the calculations made it possible to obtain quantitative agreement between the theoretical calculations and the experimental data. This interpretation of the mechanism for reactions induced by nitrogen ions in a wide range of incident energies is reasonable and completely obvious in view of the large number of open decay channels and the high level density of the compound nucleus.

However, in analyzing the differential cross sections for reactions in a wide range of particle emission angles, in Ref. 107 and later in Ref. 109 it was noticed that the angular distributions have a weakly oscillating structure. For example, in the reaction $^{12}C(^{14}N,d)^{24}Mg$ only the differential cross sections for the $5.23(3^+)$ and $7.75+7.81(1^+,5^+)$ states in ^{24}Mg (Ref. 107) have a smooth shape symmetric about 90°. The population of these states is actually not associated with the direct transfer of groups of nucleons, owing to the constraints imposed by the spin and parity selection rules. This indicates that the calculation using the statistical model of compound-nucleus formation describes only the smooth background on which are superimposed oscillations or irregularities associated with other reaction mechanisms, the contribution of which can be comparable to that of compound-nucleus formation.

There was a resurgence of interest in reactions induced by nitrogen ions after the appearance of rather contradictory data on the behavior of the $d-\alpha$ angular correlation functions in the reaction $^{12}C(^{14}N,d)^{24}Mg(\alpha)^{20}Ne$ (Refs. 14 and 15). For one of the states in ^{24}Mg, the 13.45-MeV (6^+) level, it was found[14] that there are oscillations in the ACF, whose shape is well described by the square of the sixth-order Legendre polynomial. This was interpreted as direct proof of the formation of this state via the direct transfer of 12 nucleons. Despite the fact that the results of measuring the ACFs in Ref. 15 did not reveal any oscillations and did not confirm the conclusion about a direct mechanism producing several levels in ^{24}Mg, a consensus between these experimental groups was found in joint measurements of the ACFs. These results were published recently.[16]

The measurements[16] of the $d-\alpha$ angular correlation in the reaction $^{12}C(^{14}N,d)^{24}Mg(\alpha)^{20}Ne$ for the 13.45-MeV (6^+) state in ^{24}Mg reliably confirmed the existence of oscillations in the ACFs which could not be fully explained in the compound-nucleus model. The authors interpreted their results as a manifestation of the mechanism of direct transfer of the ^{12}C nucleus in the first excited 2^+ state. The problem of theoretically explaining the ACF oscillations using the mechanism of direct mass transfer has been around for a fairly long time, and so far has not really been solved. The study of the ACFs in mass-transfer reactions is obviously one of the most promising directions in the physics of nuclear reactions.

As a first step in the systematic study of the mechanism of reactions induced by nitrogen ions, measurements were made[109] of the deuteron angular distributions in the reaction $^{12}C(^{14}N,d)^{24}Mg$, and calculations were performed in the DWBA and in the Hauser–Feshbach formalism with the parameters obtained in Ref. 107. The analysis showed that, on the average, the curves calculated using the Hauser–Feshbach model reproduce the experimental data. However, for low-lying Hauser–Feshbach levels the cross section is generally overestimated (especially at small angles), while for high-lying levels it is considerably smaller than the experimental value. Calculations performed in the EFR DWBA using the LOLA code[58] for the direct carbon-transfer mechanism showed that in this case the angular distributions possess a richer structure and in some cases more successfully

reproduce the experimental data, especially for small angles. However, no definite conclusions are possible without an estimate of the spectroscopic factors.

In Ref. 99 we extended the analysis of this reaction, using the EFR DWBA for the purpose of elevating the qualitative agreement with experiment obtained in Ref. 109 to a quantitative level and obtaining spectroscopic information. For this we estimated the reduced widths in the shell model with intermediate coupling for the $^{14}N \rightarrow {}^{12}C + d$ vertex with orbital angular momentum of the deuteron relative motion $\Lambda_2 = 0$ and 2. In general, in the EFR DWBA the amplitudes of these two states are added coherently in the matrix element (22). However, if we take into account the transfer of ^{12}C in the ground state with $I_C = 0$, the components with $\Lambda_2 = 0$ and 2 for any value of the spin I_f of the final nucleus ^{24}Mg can be added incoherently. In this case the expression for the structure factors $\theta_{l\Lambda_1\Lambda_2 I_1 I_2 I_C}$ is simplified:

$$\theta_{l\Lambda_1\Lambda_2 I_1 I_2 I_C=0} = \theta^{B\to A+C}_{\Lambda_1 I_1 I_C=0}\theta^{a\to b+C}_{\Lambda_2 I_2 I_C=0}(-1)^{l+\Lambda_1+\Lambda_2} \times \sqrt{\frac{2l+1}{(2\Lambda_1+1)(2\Lambda_2+1)}}\,\delta_{\Lambda_1 I_1}\delta_{\Lambda_2 I_2}, \tag{49}$$

where $\theta^{B\to A+C}_{\Lambda_1 I_1 I_C=0}$ and $\theta^{a\to b+C}_{\Lambda_2 I_2 I_C=0}$ are the reduced widths, which can be calculated by the methods described in Refs. 6, 33, and 34. Here the orbital angular momentum of the relative motion of the carbon nuclei Λ_1 is I_f, and the cross section is given by the sum of the partial cross sections with different transferred orbital angular momenta in accordance with the selection rules (21). Comparison of the calculated cross sections with experiment[109] gave the values of the squared reduced widths $\theta^{^{24}Mg\to{}^{12}C+{}^{12}C}_{\Lambda_1}$ for $\Lambda_1 = 0$ and 6. The calculations showed that the large values of the reduced widths for the separation of ^{12}C from Mg, and also the possibility of reproducing both the oscillatory angular distribution for the ground state and the smooth distribution (owing to the many partial cross sections with different l) for the 6^+ (13.4 MeV) state, allow a serious study of the mechanism of the $^{12}C(^{14}N,d)^{24}Mg$ reaction as the mass transfer of a large group of nucleons.

Further theoretical studies of this reaction were devoted to the more detailed determination of the contribution of the compound-nucleus mechanism and also the possibility of describing the observed oscillations of the ACFs.

For example, in Ref. 110 not only the differential cross sections, but also the angular correlation functions were analyzed in the reaction $^{12}C(^{14}N,d)^{24}Mg(\alpha)^{20}Ne$ at incident nitrogen ion energies of $E_{^{14}N} = 29$ and 35 MeV in the lab frame, in order to determine the quantitative contribution of the compound-nucleus formation mechanism.

The formalism studied in Sec. 4.2 and the CNCOR code[41] were used to calculate the spin tensors of the density matrix, the populations of magnetic sublevels of the final nuclei, and the angular correlation functions of the final particles in the statistical model of a compound nucleus.

It is well known that calculations using the statistical model of a compound nucleus are very sensitive to the choice of optical-potential parameters. Nevertheless, if the optical potentials give a good description of the angular distributions of elastically scattered particles at a given energy, the replacement of one set of parameters by another does not lead to any significant change of the transverse cross section. When the optical-potential parameters are varied the general behavior of the cross section—the forward and backward maxima, which are symmetric about $\theta = 90°$—is preserved, and only the absolute value of the differential cross section is changed by 30–40%. Our previous calculations showed that a qualitative change of the shape of the differential cross section is possible when the spin–orbit interaction parameters are varied.[40] The optical-potential parameters of Refs. 107 and 111 (see Table V) were used in these calculations.

The absolute value of the cross section calculated in the Hauser–Feshbach formalism depends most strongly on the value of $g(I)$, the total width for decay of the compound nucleus via all open channels, which, in turn, strongly depends on such parameters as the level density $\rho(E^*,I)$ and the critical angular momentum I_{cr}. The most important parameters in the calculation of $\rho(E^*,I)$ are the level-density parameter a and the pairing energies Δ. The parameter a enters into Eq. (34) inside the exponent, and so its effect is more important. For example, when a is increased by about 20%, the absolute value of the cross section decreases by more than a factor of three.

Increase of the pairing energies Δ for the most important reaction channels (the corresponding values of Δ are calculated in Refs. 45, 47, and 48) leads to an increase of the interaction cross section. Our calculations showed that an uncertainty of 1–2 MeV in the choice of the edge of the continuum E_c has little effect on the absolute value of the cross section. This is because the contribution of the continuum to the total decay width $g(I)$ significantly exceeds the contribution of the discrete spectrum and is close to the maximum allowed value. The use of Eq. (36) for estimating the yrast line leads to an uncertainty in the calculations owing to the nonuniqueness in the choice of the nuclear radius and moment of inertia. In the program we selected a model in which the nuclear moment of inertia is equal to that of a solid sphere F_s with mass mA and radius $R = 1.25A^{1/3}$ F. Some authors choose a somewhat larger nuclear radius or a moment of inertia differing slightly from F_s, for example, $R = 1.4A^{1/3}$ F and $F = 0.8F_s$ (Ref. 47) or $R = 1.5A^{1/3}$ F and $F = (0.7–0.8)F_s$ (Ref. 38). An increase of the nuclear radius leads to an increase of the moment of inertia and, consequently, to an increase in the density of high-spin levels in residual nuclei and a decrease of the interaction cross section for an individual state. However, an increase of the nuclear radius and moment of inertia will make a noticeable contribution only at high incident particle energies, when many highly excited states are formed. At low incident particle energies ($E_{c.m.} < 10$ MeV) a change of the parameters by 20–40% hardly affects the transverse cross section.

In the statistical model, an important role is played by the critical angular momentum I_{cr}, which determines the possibility of nuclear fusion in the entrance channel and the formation of a compound nucleus. It depends on the dynamics of the entrance channel and determines the maximum

TABLE V. Parameters for calculations in the Hauser–Feshbach formalism.

Channel	V, MeV	R_V, F	a_V, F	W_I, MeV	R_I, F	a_I, F	Type of potential	R_{Coul}, F	a, MeV^{-1}	Δ, MeV	Y	E_C, MeV	Number of discrete levels
$\alpha+^{22}$Na	53.15	4.33	0.58	10.80	4.33	0.580	vol.	3.36	4.00 3.67	0.00	0.194	4.36	19
$p+^{25}$Mg	53.00	3.71	0.66	6.60	3.50	0.660	vol.	3.71	4.56 4.17	2.46	0.157	5.01	18
$n+^{25}$Al	40.00	3.65	0.70	11.00	3.65	0.700	vol.	0.00	4.56 4.17	2.67	0.157	5.07	25
$d+^{24}$Mg	50.00	4.33	0.59	16.00	4.33	0.590	vol.	4.33	4.38 4.00	5.13	0.168	10.06	40
^{14}N+^{12}C	100.00	5.60	0.48	27.00	5.92	0.260	vol.	6.58					5
^{12}C+^{14}N									2.03	0.00	0.412	8.98	18
^{6}Li+^{20}Ne	65.50	4.02	0.41	12.00	3.87	1.480	vol.	6.79					14
^{20}Ne+^{6}Li													6
^{3}He+^{23}Na	11.84	5.79	0.45	1.756	5.79	0.450	vol.	5.79	3.84	1.35	0.180	5.77	19
^{5}Li+^{21}Na	11.62	6.03	0.45	1.690	6.03	0.450	vol.	6.03	3.41	2.37	0.210	5.78	35
^{8}Be+^{18}F									2.82	0.00	0.270	4.96	23
^{18}F+^{8}Be	11.67	6.24	0.45	1.700	6.24	0.450	vol.	6.24					3
^{10}B+^{16}O									3.85	2.46	0.330	8.87	6
^{16}O+^{10}B	11.07	6.31	0.45	1.510	6.31	0.450	vol.	6.31					24
^{5}He+^{21}Na	54.40	4.76	0.53	9.80	4.76	0.530	vol.	3.92	3.19	2.90	0.210	6.51	50
^{7}Be+^{19}F	35.40	4.64	1.05	11.50	5.68	0.620	sur.	6.79	2.89	1.28	0.250	4.68	15

nuclear angular momentum I_C in the reaction: $I_C=J_{cr}$.

In the channel-spin representation, the spin of the compound nucleus is determined by the selection rules (25), and so I_{cr} determines the maximum angular momentum of the nucleus I_C in a given reaction: $I_{cr}=I_C^{max}=I_1+l_a^{max}$. In order to study the sensitivity of the absolute value of the cross section to the choice of I_{cr}, the calculations were carried out for different l_a^{max}. Variations of I_{cr} affect the transverse cross section very strongly. For example, an increase of I_{cr} by $1\hbar$ leads to an increase of the cross section by about 20%. The sensitivity of the transverse cross section to I_{cr} decreases with decreasing incident particle energy. The dependence of the interaction cross section on the critical angular momentum for reactions of this type has been studied in more detail in Refs. 38, 39, and 108. In generalizing this analysis, we note that variation of the parameters of the second group leads to a change of only the absolute value of the transverse cross section, while preserving the characteristic shape of the angular distributions.

In calculating the characteristics of the reaction ^{12}C(^{14}N,d)^{24}Mg using the CNCOR code, we took into account 12 open channels via which the compound nucleus ^{26}Al could decay. These channels contribute unequally to the total decay width $g(I)$. The following four channels are the most important: $p+^{25}$Mg, $n+^{25}$Al, $\alpha+^{22}$Na, and $d+^{24}$Mg. These are the most probable decay channels for the ^{26}Al nucleus in this reaction. For the incident nitrogen energy $E_{^{14}N}=29$ MeV, the total contribution of these channels is about 98%. The relative contribution of each channel changes with increasing energy of the ^{14}N beam. For example, for $E_{^{14}N}=29$ MeV, the decay probability is distributed as follows: 19% for $\alpha+^{22}$Na, 61% for $p+^{25}$Mg, 15% for $n+^{25}$Al, and 3% for $d+^{24}$Mg. For $E_{^{14}N}=35$ MeV these values are 30% for $\alpha+^{22}$Na, 61% for $p+^{25}$Mg, 2.5% for $n+^{25}$Al, and 3.5% for $d+^{24}$Mg.

The remaining channels account for only 2%. As the energy of the incident nitrogen beam increases to 35 MeV, the contribution of these 8 channels increases by only 1%. The insignificant contribution of channels with a yield of heavy particles ^{6}Li, ^{8}Be, and so on, which can carry off a larger amount of angular momentum than light particles, is explained by the low reaction heat Q_0 and the high value of the Coulomb barrier. These channels will be closed even at relatively low excitation energy of the final nucleus, where there are only a few discrete levels. In fact, in the channel ^{6}Li+^{20}Ne, ^{20}Ne levels only up to 9.2 MeV can be populated, and in the channel ^{8}Be+^{18}F, ^{18}F levels only up to 10.4 MeV. Meanwhile, light particles can populate highly excited levels in residual nuclei, where the density of these levels is very high. Therefore, it is channels with a light-particle yield which give the dominant contribution to the total decay width $g(I)$ of a compound nucleus.

We have also estimated the probability of producing the final nucleus in both the continuum and the discrete spectrum for each channel. For a given reaction in channels where the compound nucleus decays with the emission of light particles such as p, n, d, and α, it is much more likely to produce the final nucleus in the continuum rather than in the discrete spectrum. According to our estimates, for example, in the channel $p+^{25}$Mg, this difference amounts to a factor of hundreds and even thousands. In channels where heavy nuclei are emitted, the probability of producing the final nucleus in the continuum is hundreds of times smaller than that of producing it in the discrete spectrum. For example,

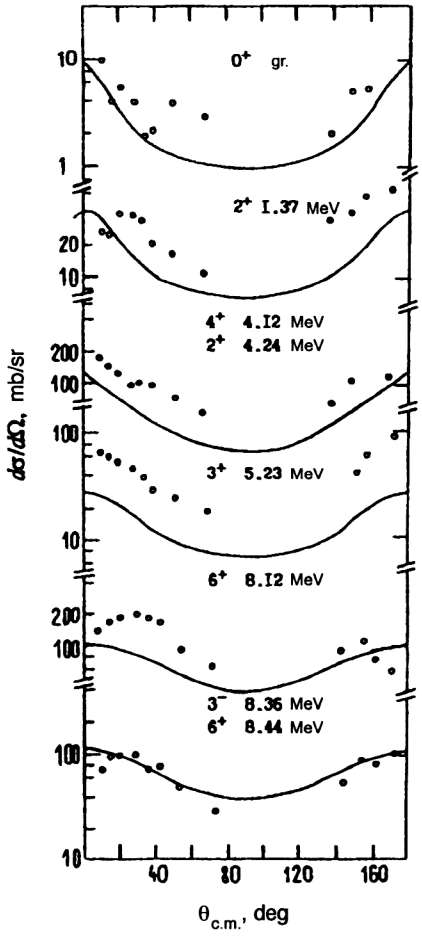

FIG. 9. Differential cross sections of the reaction $^{12}C(^{14}N,d)^{24}Mg$ for $E_{Li}=35$ MeV. The solid lines were calculated using the statistical model of compound-nucleus formation. The experimental points are from Ref. 107.

for the channel $^{8}Be+^{18}F$, the ratio of these probabilities is 1:10 at the energy $E_{^{14}N}=35$ MeV, while at $E_{^{14}N}=29$ MeV it is 1:1000.

The deuteron angular distributions in the reaction $^{12}C(^{14}N,d)^{24}Mg$ for a number of states in ^{24}Mg at $E_{^{14}N}=35$ MeV with parameters taken from Ref. 107 give a good description of experiment for the states 4.12 MeV(4^+)+4.24 MeV(2^+) and 5.23 MeV (3^+). For the other states in ^{24}Mg the calculated cross sections exceed the experimental ones. The calculation for $E_{^{14}N}=29$ MeV with the same parameters systematically exceeds experiment. This motivated us to make some changes in the model parameters in order to decrease the absolute value of the cross section. Since the angular distributions for a number of states have an oscillatory behavior, the contribution of the compound nucleus should not exceed the minima of the cross section. The best agreement with experiment at the two energies was obtained by changing two parameters: the level-density parameter a [see Eq. (34)] and the critical angular momentum of the compound nucleus I_{cr}. The combinations $a=A/5.48$ and $I_{cr}=10$ at $E_{^{14}N}=29$ MeV and 12 at $E_{^{14}N}=35$ MeV, and also $a=A/5.98$ and $I_{cr}=9$ at $E_{^{14}N}=29$ MeV and 11 at $E_{^{14}N}=35$ MeV give nearly identical results. We see from Figs. 9 and 10 that the compound-nucleus mechanism makes the largest contribution to the cross section for the reaction with formation of the ground and lowest excited states in ^{24}Mg. However, it is also clear that the theoretical curves cannot reproduce the structure of the angular distributions. For high-lying states ($E_f^*>8$ MeV), the contribution of the compound-nucleus mechanism to the cross section is smaller, despite the fact that the theoretical curves have the same smooth shape as the experimental angular distributions.

In fact, our earlier calculations using the DWBA[99] showed that the cross section for the reaction with the formation of high-lying excited states in ^{24}Mg receives a significant contribution from the mechanism of direct transfer of a group of nucleons. The magnitude of the cross section is large in this case, owing to the contribution of many partial cross sections with different angular-momentum transfers.

Therefore, our calculations of the differential cross sections in the compound-nucleus model provide additional arguments in favor of the need to consistently include both the compound-nucleus mechanism and the direct transfer of a large group of nucleons—the mass-transfer reaction.

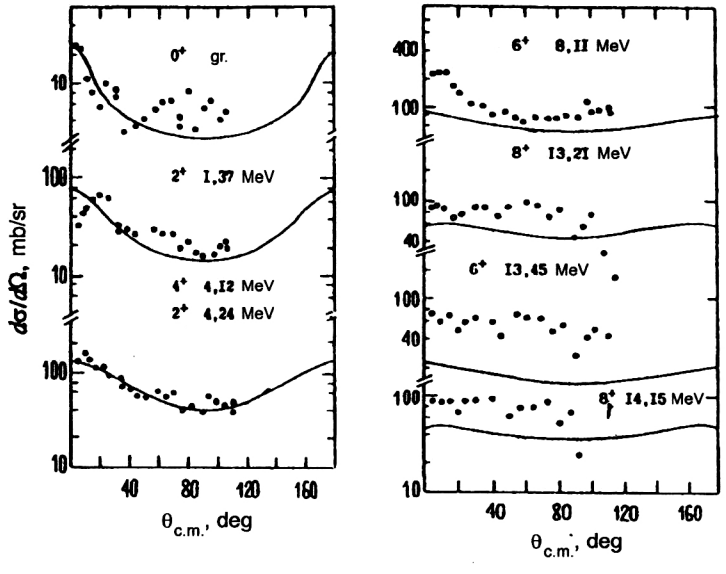

FIG. 10. Differential cross sections of the reaction $^{12}C(^{14}N,d)^{24}Mg$ for $E_{Li}=29$ MeV. The solid lines were calculated using the statistical model of compound-nucleus formation. The experimental points are from Ref. 109.

Our later studies[112] of the reaction $^{12}C(^{14}N,d)^{24}Mg$ for a number of states in ^{24}Mg using the EFR DWBA showed that a special feature of the direct-transfer mechanism in this reaction is that enhancement of the excitation of the final ^{24}Mg nucleus strongly enhances the peripheral nature of the process. In the DWBA calculations this is manifested in the rather inaccurate description of the behavior of the wave functions of the cluster relative motion inside the nucleus at small r. In this case it becomes necessary to cut off small values of the orbital partial waves in the entrance and exit channels. Calculation of the $d-\alpha$ angular correlation function using the EFR DWBA with the two-component wave function of ^{14}N with relative angular momenta equal to 0 and 2 and with the reduced widths calculated in the shell model allowed the observed oscillations of the ACFs to be reproduced for direct transfer of the ^{12}C nucleus in the ground state.

7. STUDY OF THE POLARIZATION TENSORS OF LIGHT NUCLEI BY THE PARTICLE–PARTICLE CORRELATION METHOD

This section is devoted to the use of the particle angular correlations for directly reconstructing the components of the spin density matrix, the spin tensors, or the polarization tensors from the experimental data, and also to the theoretical analysis of these results.

Experimental studies of the polariztaion tensors of the final nucleus were performed for the reaction $^{13}C(p,d)^{12}C^*(15.11\ \text{MeV},1^+)\rightarrow{}^{12}C(\text{g.s.})$ by measuring the $d-^{12}C$ correlation,[23] and also by studying inelastic scattering[24] and heavy-ion transfer reactions.[74]

Experimental and theoretical studies of the polarization tensor of the final nucleus $^6Li^*(2.186\ \text{MeV},3^+)$ from the $^9Be(p,\alpha_1)^6Li$ reaction at $E_p=40$ MeV were performed in Ref. 113. This state, which has a width of 0.024 MeV, decays into a deuteron and an α particle, which makes it possible to measure the functions describing the angular correlation between α_1 and α-particle decay.

Equation (13) for the angular correlation function $W(\Omega_b,\Omega_c)$ can be written as

$$W(\Omega_b,\Omega_c)=\sum_{k\varkappa} t_{k\varkappa}(\theta_b)\left(\frac{4\pi}{2k+1}\right)^{1/2} A_k Y^*_{k\varkappa}(\theta_c) \qquad (50)$$

after determining the polarization tensors $t_{k\varkappa}(\theta_b)$ as the spin tensors of the density matrix $\rho_{k\varkappa}$ normalized to the first element ρ_{00}. The polarization tensors are usually measured in the plane perpendicular to the reaction plane. In (50) the constants A_k are the components of the efficiency tensor (16) normalized to the first element ε_{00}. According to the angular-momentum addition rules (14), the following values of the angular momentum are possible in the decay of the 3^+ state into a deuteron and an α particle: the channel spin S equal to 1, and the orbital angular momentum of the relative motion of the decay products $l=2$ or 4, $k<6$. It is assumed that the contribution of $l=4$ is much smaller than that of $l=2$. Then k takes values no greater than 4, and the constants A_k have the values $A_0=1$, $A_2=-0.99$, and $A_4=0.67$. It follows from the symmetry laws and the definition of the polarization tensor that $t_{00}=1$ and $t_{k\varkappa}=0$ for odd k, $t^*_{k\varkappa}=(-1)^{\varkappa}t_{k-\varkappa}$.

Since measurements in a single plane of the decay fragments are insufficient for determining the polarization tensor of the nucleus in the 3^+ state, the fragments were recorded using two detectors arranged horizontally in the reaction plane and two detectors arranged perpendicular to this plane. The angular correlation function (50) is a linear combination of spherical harmonics $Y_{k\varkappa}$, and so processing of the experimental angular dependences of the ACFs using the Monte Carlo method allowed the extraction of the desired components of the polarization tensor. Independent measurement of the differential cross sections of the $^9Be(p,\alpha)^6Li$ reaction for the ground and excited states of ^6Li made it possible to perform a complete theoretical analysis of these results.

The calculations[113] were carried out on the basis of the EFR DWBA formalism using the OLYMP code.[41] The differential cross section for the inverse reaction $^6Li(\alpha,p)^9Be$ at $E_\alpha=20.7$ MeV which we calculated earlier in Ref. 101 showed that all four of the single-stage direct mechanisms play an important role in this reaction. Therefore, in analyzing the polarization, the contribution of direct processes (cluster stripping–pickup and heavy substitution) and exchange processes (heavy stripping–pickup and substitution) was determined using the reduced widths calculated in the shell model with intermediate coupling.

Figure 11, where we compare the theoretical differential cross sections (solid lines) with the experimental data (circles), shows that for the ground state, direct processes contribute to the cross section at forward angles ($\theta_\alpha<60°$) of the α-particle emission, while exchange processes dominate for angles $\theta_\alpha>60°$. This result, which is analogous to that obtained in Ref. 101, indicates a large probability for the $(\alpha+^5He)$-cluster configuration in the ground state of ^9Be. A characteristic feature of the calculated differential cross sections is their weak sensitivity to significant changes of the model parameters, especially to the choice of parameters of the wave functions of the relative motion. The interference of states with different angular momenta Λ_1 of the relative motion at the $^9Be\rightarrow\alpha+^5He$ vertex is important in calculating exchange processes. The destructive interference of the amplitudes with $\Lambda_1=0$ and 2 due to the reduced widths of opposite signs leads to a decrease of the total cross section relative to the contribution of each of these states separately.

The differential cross section for the (2.186 MeV, 3^+) state is mainly determined by direct processes. Exchange processes contribute only at angles $\theta_\alpha>120°$. The diminished relative importance of exchange processes for the 3^+ state relative to the ground state of ^6Li is related, first of all, to the decrease of the reduced widths for amplitudes with orbital angular-momentum transfer $l=3$, which give the main contribution to the cross section. Another feature of this reaction is the need to cut off the partial distorted-wave expansion in the $p+^9Be$ channel in the angular momentum L_a, owing to the surface nature of the reaction. The cutoff of small partial waves with $L_a<3$ has little effect on the shape of the differential cross sections, but leads to a change of the relative importances of the pickup and substitution mecha-

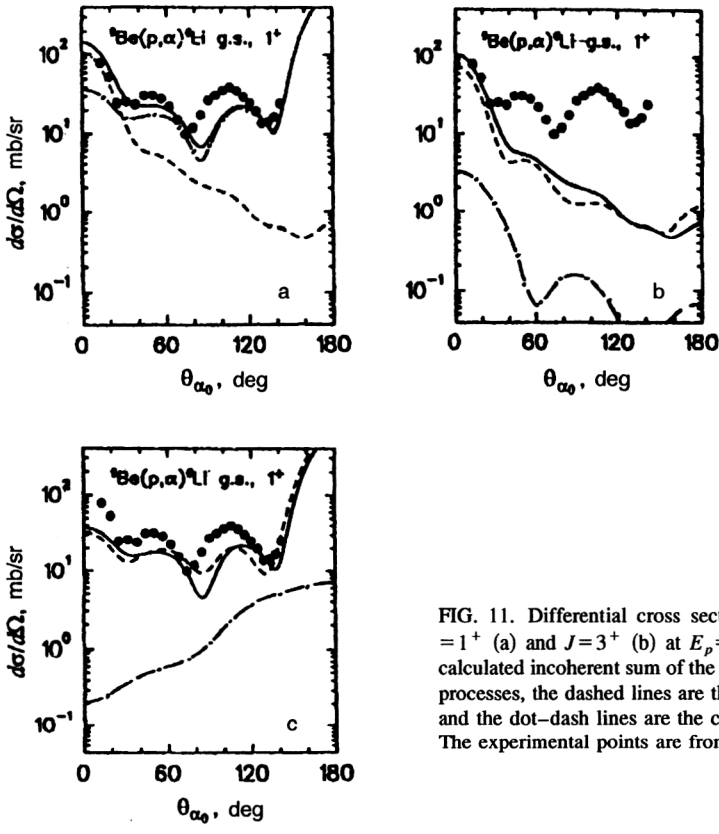

FIG. 11. Differential cross section of the reaction ^{9}Be$(p,\alpha)^6$Li, $J=1^+$ (a) and $J=3^+$ (b) at $E_p=40$ MeV. The solid lines show the calculated incoherent sum of the cross sections for direct and exchange processes, the dashed lines are the cross sections for direct processes, and the dot–dash lines are the cross sections for exchange processes. The experimental points are from Ref. 114.

nisms, and also is clearly manifested in the calculation of the angular dependences of the polarization tensor.

The relative importances of the triton-pickup and heavy-substitution (inclusion of proton rescattering on ^{6}Li) mechanisms in the reaction with formation of the ^{6}Li ground state and the 3^+ state are changed. For the ground state, heavy substitution is suppressed by an order of magnitude compared to pickup. The contribution of heavy substitution to the reaction cross section for the 3^+ state is, as seen from Fig. 12, very important, and the contribution of the interference term is comparable in magnitude to the pickup contribution.

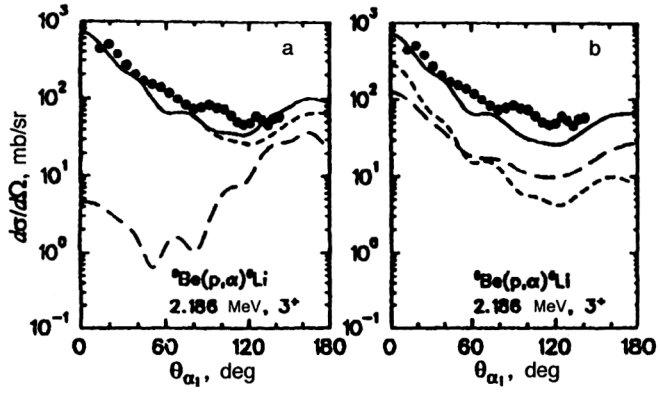

FIG. 12. Differential cross section of direct processes in the reaction ^{9}Be$(p,\alpha)^6$Li, $J=3^+$ at $E_p=40$ MeV. The solid line is the coherent sum of the amplitudes for the stripping and heavy-substitution mechanisms, the dotted line is the cross section for the stripping mechanism, and the dashed line is the cross section for the heavy-substitution mechanism. The experimental points are from Ref. 114.

This may be a reflection of the difference of the cluster structure of the excited state (2.186 MeV, 3^+) in ^{6}Li from that of the ground state of ^{6}Li.

The theoretical analysis of the polarization tensors of excited states of light nuclei and, in particular, ^{6}Li gives more information about the structure of these states and the reaction dynamics than does analysis of the differential cross sections. This is not only because of the large number of angular distributions studied, but, mainly, because the angular dependences of the components $t_{k\varkappa}$ are highly sensitive to the model parameters. This feature of the polarization tensors (and, as noted above, the spin tensors of the density matrix) is related to the coherent summation over the transferred orbital angular momentum l and the incoherent summation over the total transferred spin s and channel spin j. The use of these intermediate angular momenta, defined by the selection rules

$$\mathbf{s}=\mathbf{S}_a+\mathbf{S}_b, \quad \mathbf{j}=\mathbf{I}_f+\mathbf{l}=\mathbf{I}_A+\mathbf{s},$$

instead of the angular momenta I_1 and I_2 is convenient for reactions induced by particles no heavier than ^{4}He, when the total angular momenta I_a and I_b are replaced by their spins S_a and S_b. Then, instead of coherent summation over I_1 and I_2 in the expression for the spin tensors (23), we have incoherent summation over s and j. In particular, for the ^{9}Be$(p,\alpha)^6$Li reaction, $s=1/2$ and $j=1$ and 2.

In Fig. 13 we show the experimental and theoretical angular distributions of the components of the polarization tensor of the (2.186 MeV, 3^+) state in ^{6}Li. Since the data for $t_{k\varkappa}(\theta_\alpha)$ have been obtained only for $\theta_\alpha<80°$, the theoretical curves take into account the contribution of only direct pro-

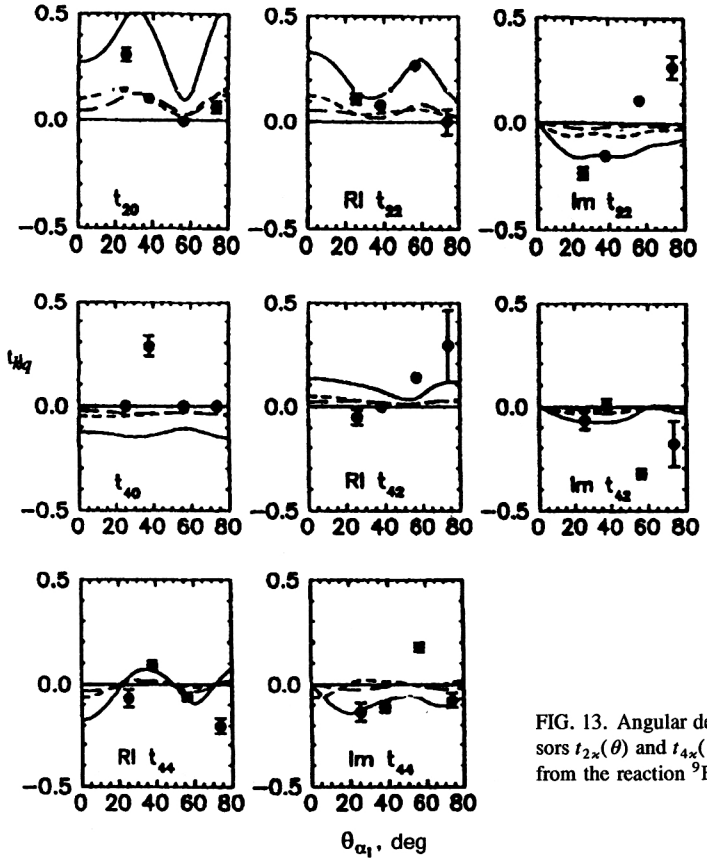

FIG. 13. Angular dependences of the components of the polarization tensors $t_{2\varkappa}(\theta)$ and $t_{4\varkappa}(\theta)$ of the ^{6}Li nucleus in the 3^+, $E^*=2.186$ MeV state from the reaction ^{9}Be$(p,\alpha)^6$Li.

cesses (the contribution of exchange processes is very small at these angles), including the coherent sum of capture and heavy substitution.

The theoretical analysis showed that the angular distributions of the components of the polarization tensor are very sensitive to the parameters of the wave function of the relative motion $\Psi_{^9\text{Be}\to^6\text{Li}(3^+)+t}$. A fit of the parameters of this function describing the relative motion of t and ^{6}Li in the 3^+ state of ^{9}Be showed that it differs significantly from the corresponding function for $^6\text{Li}_{\text{g.s.}}$ and from the shell-model predictions. In particular, it is more extended and contains more nodes. The reduced widths extracted by comparing the calculated and experimental distributions also differ slightly from the model ones.

The difficulties in describing the angular dependence of the leading component of the polarization tensor t_{20} were overcome by cutting off small partial-wave angular momenta L_a in the $p+^9$Be channel. The contribution of these angular momenta significantly distorted the angular dependences and shifted the experimentally observed oscillations. Unfortunately, the description of the angular dependences of the imaginary part of the components $t_{k\varkappa}$ with $k=4$ becomes much worse. This is perhaps a consequence of the need to include the spin–orbit interaction, the effect of which on the imaginary part of the polarization tensor can be very strong.

CONCLUSION

We conclude by emphasizing that the particle–particle angular correlations in the excitation of a particular level of the final nucleus always describe only aligned systems, because k is always even. Nevertheless, the study of such correlations is interesting from the viewpoint of the ability of the ACFs to select the type of decaying state, because the angular correlations prove to be sizable only if the wave function of the state possesses a large probability (reduced width) for decay via the given channel.

Therefore, the particle–particle angular correlation functions should be especially sensitive not only to the reaction mechanism, but also to the form of the wave functions. In particular, when studying the ACFs of particles produced in the decay of high-lying states, it is necessary to have an accurate description of the wave functions of quasistationary states. One method of doing this, the computer modeling of wave functions of the Gamow type, has been described in this review.

Another feature of the study of the ACFs in reactions involving semiheavy ions and the study of strongly excited nuclear states is the need to correctly calculate the overlap integrals in the interior of the nucleus. The standard approaches in DWBA calculations often tend to overestimate the role of the nuclear interior. The cases studied here, where a cutoff is introduced for small orbital partial waves, have led to significant progress in the interpretation of some of the experimental data.

The difficulties arising in the description of the angular dependences of the imaginary parts of the components of the polarization tensors indicate that it is necessary to include the spin–orbit interaction, which can very strongly affect the imaginary part of the polarization tensor.

[1] L. C. Biedenharn and M. E. Rose, Rev. Mod. Phys. **25**, 729 (1953).
[2] U. Fano, Phys. Rev. **90**, 577 (1953).
[3] F. Coester and J. M. Jauch, Helv. Phys. Acta **26**, 3 (1953).
[4] L. Goldfarb, in *Angular Correlation and Polarization*, Vol. 1: *Nuclear Reactions*, edited by P. M. Endt and M. Demer [Russ. transl., IIL, Moscow, 1962].
[5] O. F. Nemets and A. M. Yasnogorodskiĭ, *Polarization Phenomena in Nuclear Physics* [in Russian] (Naukova Dumka, Kiev, 1980).
[6] N. S. Zelenskaya and I. B. Teplov, *Characteristics of Excited States of Nuclei and Angular Correlations in Nuclear Reactions* [in Russian] (Énergoatomizdat, Moscow, 1955).
[7] H. Tyren, P. Hillman, and Th. A. Maris, Nucl. Phys. **7**, 10 (1958).
[8] V. V. Balashov and A. N. Bojarkina, Nucl. Phys. **38**, 629 (1962).
[9] P. Beregi, N. S. Zelenskaya, V. G. Neudatchin, and Ju. F. Smirnov, Nucl. Phys. **66**, 513 (1965).
[10] V. I. Komarov, Fiz. Élem. Chastits At. Yadra **5**, 419 (1974) [Sov. J. Part. Nucl. **5**, 168 (1975)].
[11] K. P. Artemov, V. Z. Goldberg, I. A. Petrov *et al.*, Phys. Lett. B **37**, 61 (1971).
[12] A. A. Ogloblin, Fiz. Élem. Chastits At. Yadra **3**, 936 (1972) [Sov. J. Part. Nucl. **3**, 467 (1972)].
[13] A. D. Panagiotou, J. C. Cornell, N. Anyas-Weiss *et al.*, J. Phys. **7**, 1748 (1974).
[14] K. P. Artemov, V. Z. Goldberg, M. S. Golovkov *et al.*, Phys. Lett. B **149**, 325 (1984).
[15] A. H. Wuosmaa, S. Saini, P. H. Kutt *et al.*, Phys. Lett. B **172**, 297 (1986).
[16] R. W. Zurmuhle, Z. Liu, D. R. Benton *et al.*, Phys. Rev. C **49**, 2549 (1994).
[17] N. S. Zelenskaya and I. B. Teplov, Izv. Akad. Nauk SSSR, Ser. Fiz. **44**, 960 (1980) [Bull. Acad. Sci. USSR, Phys. Ser.].
[18] N. S. Zelenskaya and I. B. Teplov, Nucl. Phys. A **406**, 306 (1983).
[19] N. S. Zelenskaya and I. B. Teplov, Fiz. Élem. Chastits At. Yadra **18**, 1283 (1987) [Sov. J. Part. Nucl. **18**, 546 (1987)].
[20] O. I. Vasil'eva, G. S. Gurevich, A. V. Ignatenko *et al.*, Yad. Fiz. **45**, 312 (1987) [Sov. J. Part. Nucl. **45**, 195 (1987)]; **49**, 625 (1989) [**49**, 387 (1989)].
[21] A. B. Ignatenko, V. M. Lebedev, N. V. Orlova *et al.*, Izv. Akad. Nauk SSSR, Ser. Fiz. **52**, 996 (1988) [Bull. Acad. Sci. USSR, Phys. Ser.]; Izv. Ross. Akad. Nauk, Ser. Fiz. **58**, 188 (1994) [Bull. Russ. Acad. Sci., Phys. Ser.]; **60**, 189 (1996); Yad. Fiz. **55**, 597 (1992) [Sov. J. Nucl. Phys. **55**, 330 (1992)]; **57**, 195 (1994) [Phys. At. Nucl. **57**, 181 (1994)]; **58**, 208 (1995) [**58**, 166 (1995)].
[22] J. R. Campbell, W. R. Falk, N. E. Davison *et al.*, Nucl. Phys. A **470**, 349 (1987).
[23] P. Wust, W. Von Oertzen, H. Ossenbrink *et al.*, Phys. Lett. B **80**, 208 (1979).
[24] *A Theoretical Practicum in Nuclear Physics*, edited by V. V. Balashov [in Russian] (Énergoatomizdat, Moscow, 1984).
[25] K. Blum, *Density Matrix Theory and Its Applications* (Plenum Press, New York, 1981) [Russ. transl., Mir, Moscow, 1983].
[26] L. C. Biedenharn and J. D. Louck, *Angular Momentum in Quantum Mechanics* (Addison-Wesley, Reading, Mass., 1981) [Russ. transl., Mir, Moscow, 1984].
[27] E. Sheldon, Rev. Mod. Phys. **35**, 795 (1963).
[28] W. Tobocman, *Theory of Direct Nuclear Reactions* (Oxford University Press, Oxford, 1961).
[29] T. Tamura, Phys. Rep. **14**, 59 (1974).
[30] N. Austern, Phys. Rev. **136**, 1743 (1964).
[31] G. R. Satchler, Nucl. Phys. **55**, 1 (1964).
[32] N. Austern, R. M. Drisko, E. C. Halbert, and G. R. Satchler, Phys. Rev. **133**, 3 (1964).
[33] N. S. Zelenskaya and I. B. Teplov, Fiz. Élem. Chastits At. Yadra **11**, 342 (1980) [Sov. J. Part. Nucl. **11**, 126 (1980)].
[34] N. S. Zelenskaya and I. B. Teplov, *Exchange Processes in Nuclear Reactions* [in Russian] (Moscow State University Press, Moscow, 1985).
[35] H. Feshbach and V. I. Weisskopf, Phys. Rev. **76**, 1550 (1949).
[36] L. Wolfenstein, Phys. Rev. **82**, 690 (1951).
[37] W. Hauser and H. Feshbach, Phys. Rev. **87**, 366 (1952).
[38] D. L. Hanson, R. G. Stokstad, K. A. Erb *et al.*, Phys. Rev. C **9**, 929 (1974).
[39] S. K. Penny, *The FORTRAN Program HELGA* (unpublished).
[40] N. A. Bogdanova, N. S. Zelenskaya, and I. B. Teplov, Yad. Fiz. **51**, 986 (1990) [Sov. J. Nucl. Phys. **51**, 631 (1990)].
[41] T. L. Belyaeva, N. S. Zelenskaya, and N. V. Odinsov, Comput. Phys. Commun. **73**, 161 (1992).
[42] T. L. Belyaeva, N. S. Zelenskaya, L. Z. Ismail *et al.*, *A Computer Program For Calculating the Cross Sections and Phase Shifts of the Elastic Scattering of Particles With Spin in the Optical Model. Analysis and Interpretation of Physical Experiments* [in Russian] (Moscow State University Press, Moscow, 1979), p. 84.
[43] T. L. Belyaeva, N. A. Bogdanova, N. S. Zelenskaya, and N. V. Odintsov, Preprint 92-40/289, Institute of Nuclear Physics, Moscow State University (1992) [in Russian].
[44] F. Ajzenberg-Selove, Nucl. Phys. A **460**, 1 (1986); **475**, 1 (1987).
[45] H. Bethe, Phys. Rev. **50**, 332 (1936).
[46] V. A. Kravtsov, *Atomic Masses and Nuclear Binding Energies* [in Russian] (Atomizdat, Moscow, 1974).
[47] A. Gilbert and A. G. Cameron, Can. J. Phys. **43**, 1446 (1965).
[48] A. Gilbert, F. S. Chen, and A. G. Cameron, Can. J. Phys. **43**, 1248 (1965).
[49] K. Bethge, K. Meier-Ewert, K. O. Pfeiffer, and R. Bock, Phys. Lett. B **24**, 663 (1967).
[50] R. Middleton, B. Rosner, D. J. Pullen, and L. Polsky, Phys. Rev. Lett. **20**, 118 (1968).
[51] V. Z. Gol'dberg, V. V. Davydov, A. A. Ogloblin *et al.*, Izv. Akad. Nauk SSSR, Ser. Fiz. **33**, 566 (1969) [Bull. Acad. Sci. USSR, Phys. Ser.].
[52] N. Anyas-Weiss, J. C. Cornell, P. S. Fisher *et al.*, Phys. Rep. **12**, 201 (1974).
[53] O. F. Nemets, V. G. Neudachin, A. T. Rudchik *et al.*, *Nucleon Associations in Nuclei and Multinucleon Transfer Reactions* [in Russian] (Naukova Dumka, Kiev, 1989).
[54] M. C. Mallet-Lemaire, in *Proceedings of the Conf. on Clustering Aspects of Nuclear Structure and Nuclear Reactions*, Winnipeg, 1978, AIP Conf. Proc. No. 47, p. 271.
[55] L. R. Greenwood, R. E. Segel, K. Raghunatan *et al.*, Phys. Rev. C **12**, 156 (1975).
[56] H. S. Bradlow, W. D. M. Rae, P. S. Fisher *et al.*, Nucl. Phys. A **314**, 171, 207 (1979).
[57] L. A. Charlton and D. Robson, Bull. Am. Phys. Soc. **17**, 508 (1972).
[58] R. M. De Vries, *The Computer Code LOLA*, Saclay (1974).
[59] T. Tamura and R. S. Low, Chem. Phys. **8**, 349 (1974).
[60] T. L. Belyaeva, P. N. Zaikin, N. S. Zelenskaya *et al.*, *The OLYMP Code For Calculating the Cross Sections of Reactions Involving Complex Particles by the Distorted Wave Method with Finite Interaction Range* [in Russian] (Moscow State University Press, Moscow, 1981).
[61] A. T. Rudchik, V. N. Dobrikov, O. Yu. Goryunov *et al.*, Yad. Fiz. **34**, 306 (1981) [Sov. J. Nucl. Phys. **34**, 173 (1981)].
[62] Yu. A. Kudeyarov, I. V. Kurdyumov, V. G. Neudatchin, and Yu. F. Smirnov, Nucl. Phys. A **163**, 316 (1971).
[63] V. M. Krasnopol'skiĭ and V. I. Kukulin, Yad. Fiz. **20**, 883 (1974) [Sov. J. Nucl. Phys. **20**, 470 (1975)].
[64] V. I. Kukulin, V. G. Neudachin, and V. N. Pomerantsev, Yad. Fiz. **24**, 298 (1976) [Sov. J. Nucl. Phys. **24**, 155 (1976)].
[65] J. S. Bergstrom, Nucl. Phys. A **327**, 458 (1979).
[66] V. I. Kukulin, V. M. Krasnopolsky, V. T. Voronchev, and P. B. Sazonov, Nucl. Phys. A **417**, 128 (1984).
[67] H. Kanada, T. Kanenko, S. Saito, and Y. C. Tang, Nucl. Phys. A **444**, 209 (1985).
[68] K. Meier-Ewert, K. Bethge, and K. P. Pfeiffer, Nucl. Phys. A **110**, 142 (1968).
[69] F. Puhlhofer, H. G. Ritter, R. Bock *et al.*, Nucl. Phys. A **147**, 258 (1970).
[70] K. I. Kubo and M. Hirata, Nucl. Phys. A **187**, 186 (1972).
[71] M. E. Cobern, D. J. Pisano, and P. D. Parker, Phys. Rev. C **14**, 491 (1976).
[72] F. D. Becchetti, E. R. Flynn, D. L. Hanson, and J. W. Sunier, Nucl. Phys. A **305**, 293 (1978).
[73] M. Avril, M. Lepareux, N. Saunier *et al.*, J. Phys. (Paris) **36**, 229 (1975).
[74] F. Paugheon, P. Raussel, M. Bernas *et al.*, Nucl. Phys. A **325**, 481 (1979).
[75] K. R. Artemov, V. Z. Gol'dberg, I. P. Petrov *et al.*, Yad. Fiz. **21**, 1157 (1975) [Sov. J. Nucl. Phys. **21**, 596 (1975)]; **22**, 242 (1975) [**22**, 125 (1975)]; **23**, 489 (1976) [**23**, 257 (1976)].
[76] K. R. Artemov, V. Z. Gol'dberg, I. P. Petrov *et al.*, Yad. Fiz. **21**, 1169 (1975) [Sov. J. Nucl. Phys. **21**, 603 (1975)].
[77] K. R. Artemov, V. Z. Gol'dberg, and M. S. Golovkov, Yad. Fiz. **37**, 1351 (1983) [Sov. J. Nucl. Phys. **37**, 805 (1983)].
[78] M. C. Etchegoyen, D. Sinclair, A. Etchegoyen *et al.*, Nucl. Phys. A **402**, 87 (1983).
[79] M. S. Golovkov, V. Z. Gol'dberg, A. D. Sidorenko *et al.*, Yad. Fiz. **38**, 284 (1983) [Sov. J. Nucl. Phys. **38**, 168 (1983)].

[80]E. F. Da Silveira, Thesis No. 1825, Orsay (1977).
[81]K. R. Artemov, M. S. Golovkov, V. Z. Gol'dberg *et al.*, Yad. Fiz. **46**, 1331 (1987) [Sov. J. Nucl. Phys. **46**, 782 (1987)].
[82]T. L. Belyaeva and N. S. Zelenskaya, Ukr. Fiz. Zh. **34**, 1635 (1989) [in Russian].
[83]K. R. Artemov, M. S. Golovkov, V. Z. Gol'dberg *et al.*, Yad. Fiz. **48**, 935 (1988) [Sov. J. Nucl. Phys. **48**, 596 (1988)].
[84]E. F. Da Silveira, in *Proceedings of the Fourteenth Winter Meeting on Nuclear Physics*, Bormio, 1976.
[85]T. L. Belyaeva, N. S. Zelenskaya, and I. B. Teplov, State Archives of Algorithms and Computer Programs, No. 50850000734 (1985) [in Russian].
[86]B. Buck and P. E. Hodson, Philos. Mag. **6**, 1371 (1961).
[87]T. L. Belyaeva, N. S. Zelenskaya, and N. V. Odintsov, Yad. Fiz. **56**, No. 9, 50 (1993) [Phys. At. Nucl. **56**, 1179 (1993)].
[88]G. A. Gamow, Z. Phys. **51**, 204 (1928).
[89]A. I. Baz', Ya. B. Zel'dovich, and A. M. Perelomov, *Scattering, Reactions and Decay in Nonrelativistic Quantum Mechanics*, transl. of 1st Russ. ed. (Israel Program for Scientific Translations, Jerusalem, 1966) [Russ. original, 2nd ed., Nauka, Moscow, 1971].
[90]R. Huby and J. R. Mines, Rev. Mod. Phys. **37**, 406 (1965).
[91]V. B. Subbotin, V. M. Semjonov, K. A. Gridnev, and E. F. Hefter, Phys. Rev. C **28**, 1618 (1983).
[92]C. M. Vincent and H. T. Fortune, Phys. Rev. C **2**, 782 (1970).
[93]A. Arima and S. Yoshida, Phys. Lett. B **40**, 15 (1972).
[94]S. G. Kadmenskiĭ and V. I. Furman, *Alpha Decay and Related Nuclear Reactions* [in Russian] (Énergoatomizdat, Moscow, 1985).
[95]P. Schumacher, N. Ueta, H. H. Duhm *et al.*, Nucl. Phys. A **212**, 573 (1973).
[96]L. S. Dennis, A. Roy, A. D. Frawley, and K. W. Kemper, Nucl. Phys. A **359**, 455 (1981).
[97]J. D. Garret and O. Hansen, Nucl. Phys. A **212**, 600 (1973).
[98]H. V. Klapdor, H. Reiss, and G. Rosner, Nucl. Phys. A **262**, 157 (1976).
[99]T. L. Belyaeva and N. S. Zelenskaya, Izv. Akad. Nauk SSSR, Ser. Fiz. **52**, 942 (1988) [Bull. Acad. Sci. USSR, Phys. Ser.].
[100]K. F. Pal, R. G. Lovas, M. A. Nagarajan *et al.*, Nucl. Phys. A **402**, 114 (1983).
[101]T. L. Belyaeva, N. S. Zelenskaya, and I. B. Teplov, Yad. Fiz. **38**, 901 (1983) [Sov. J. Nucl. Phys. **38**, 540 (1983)].
[102]A. K. Kerman and K. W. McVoy, Ann. Phys. (N.Y.) **122**, 197 (1979).
[103]T. Udagawa and T. Tamura, Phys. Rev. Lett. **45**, 13 (1980).
[104]N. Marquardt, J. D. Garret, and H. T. Fortune, Phys. Lett. B **35**, 37 (1971).
[105]K. Nagatani, M. J. LeVine, T. A. Belote, and A. Arima, Phys. Rev. Lett. **27**, 1071 (1971).
[106]T. H. Belote, N. Anyas-Weiss, J. A. Becker *et al.*, Phys. Rev. Lett. **30**, 450 (1973).
[107]C. Volant, M. Conjeaud, S. Harar *et al.*, Nucl. Phys. A **238**, 120 (1975).
[108]H. V. Klapdor, H. Reiss, G. Rosher, and M. Schrader, Nucl. Phys. A **244**, 157 (1975).
[109]K. R. Artemov, M. S. Golovkov, V. Z. Gol'dberg *et al.*, Yad. Fiz. **44**, 579 (1986) [Sov. J. Nucl. Phys. **44**, 373 (1986)].
[110]T. L. Belyaeva, N. S. Zelenskaya, and N. V. Odintsov, Izv. Ross. Akad. Nauk, Ser. Fiz. **58**, 112 (1994) [Bull. Acad. Sci. USSR, Phys. Ser.].
[111]C. M. Perrey and F. G. Perrey, At. Data Nucl. Data Tables **17**, 1 (1976).
[112]T. L. Belyaeva, N. S. Zelenskaya, and N. V. Odintsov, *Abstracts of Reports Presented at the Forty-Third Meeting on Nuclear Spectroscopy and Structure of the Atomic Nucleus* [in Russian] (Institute of Nuclear Physics, St. Petersburg, 1993), p. 306.
[113]T. L. Belyaeva and N. S. Zelenskaya, *Abstracts of Reports Presented at the Forty-Fifth Meeting on Nuclear Spectroscopy and Structure of the Atomic Nucleus* [in Russian] (Institute of Nuclear Physics, St. Petersburg, 1995), p. 308.
[114]W. R. Falk, Private report (1995).

Translated by Patricia A. Millard